

Space Experiments with Particle Accelerators (SEPAC):

Description of Instrumentation

by

W.W.L. Taylor  
TRW  
Redondo Beach, CA 90278

W.T. Roberts, D.L. Reasoner, C.R. Chappell, B.B. Baker,  
J. Watkins  
Marshall Space Flight Center  
Huntsville, AL 35812

J.L. Burch, W.C. Gibson, R.K. Black, W.M. Tomlinson,  
G.A. Ferguson  
Southwest Research Institute  
San Antonio, TX 78284

J.R. Bounds, W.M. Womack  
General Digital, Inc.  
Huntsville, AL 35805

P.M. Banks, P.R. Williamson, T. Neubert  
Stanford University  
Stanford, CA 94305

W.S. Williamson  
Hughes Research Laboratories  
Malibu, CA 90265

T. Obayashi, M. Nagatomo, N. Kawashima, K. Kuriki,  
K. Ninomiya, S. Sasaki, M. Yanagisawa  
Institute for Space and Astronautical Science  
Tokyo, Japan

M. Ejiri  
National Institute of Polar Research  
Tokyo, Japan

I. Kudo  
Electro-Technical Laboratories  
Tokyo, Japan

December 1987

(NASA-TM-89728) SPACE EXPERIMENTS WITH  
PARTICLE ACCELERATORS (SEPAC): DESCRIPTION  
OF INSTRUMENTATION (NASA) 68 p CSCL 04A

N88-21606

Unclas  
G3/46 0137323

## Abstract

SEPAC (Space Experiments with Particle Accelerators) flew on SL 1 (Spacelab 1) in November-December 1983. SEPAC is a joint U.S.-Japan investigation of the interaction of electron, plasma, and neutral beams with the ionosphere, atmosphere, and magnetosphere. It is scheduled to fly again on ATLAS 1 in August 1990. On SL 1, SEPAC used an electron accelerator, a plasma accelerator, and a neutral gas source as active elements and an array of diagnostics to investigate the interactions. For ATLAS 1, the plasma accelerator will be replaced by a plasma contactor and charge collection devices to improve vehicle charging neutralization. This paper describes the SEPAC instrumentation in detail for the SL 1 and ATLAS 1 flights and includes a bibliography of SEPAC papers.

## 1.0 INTRODUCTION

Injections of electron beams, plasmas and neutral gases into the ionosphere have been performed for many years (see Meriwether, et al., 1973; Israelson and Winckler, 1979; Annales de Geophysique, 1980; Winckler, 1980; Grandal, 1982; Banks, et al., 1982; Kintner and Kelley, 1982; Radio Science, 1984; and Shawhan, et al., 1984).

SEPAC (Space Experiments with Particle Accelerators) is a comprehensive Spacelab facility designed to actively probe the ionosphere, atmosphere, and magnetosphere with electron and plasma accelerators. The instrumentation includes diagnostics to sense changes in these portions of space. It was developed for Spacelab 1 as a joint U.S.-Japan program under the leadership of one of the authors, T. Obayashi, Principal Investigator.

The scientific objectives of the SEPAC investigation are to:

- o Study the interaction of electron and plasma beams with plasmas.
- o Produce artificial aurora to measure quantitatively the efficiencies of auroral light.
- o Measure the morphology of the Earth's magnetic and electric fields.
- o Determine the possible modification of the Earth's ionosphere.
- o Study spacecraft charging.

SEPAC flew on Spacelab 1 from November 28 to December 8, 1983. Initial results of the SEPAC flight on SL 1 are described by Obayashi, et al. (1984) and Taylor, et al. (1985). The

bibliography lists SEPAC papers. A number of other investigations flew on SL 1 which provided additional diagnostic data for SEPAC. Atmospheric Emissions Photometric Imager (AEPI) is a sensitive optical device designed to measure emissions from artificial and natural sources (Mende, et al., 1984). A low energy electron spectrometer and magnetometer on SL 1 provided valuable data, especially on the returning electrons (Wilhelm, et al., 1984). PICPAB (Phenomena Induced by Charged Particle Beams) included low intensity electron and ion accelerators as well as diagnostics (Beghin, et al., 1984).

SEPAC is scheduled to fly again on ATLAS 1 (Atmospheric Laboratory for Applications and Science) in August 1990. Improvements and other modifications will be made before this flight. The purpose of this paper is to describe SEPAC instrumentation as it flew on Spacelab 1 and as it will fly on ATLAS 1.

## 2.0 INSTRUMENTATION OVERVIEW

The active portions of SEPAC as it flew on SL 1 were the electron beam accelerator (EBA), the magnetoplasma dynamic arcjet (MPD-AJ), and the neutral gas plume (NGP). The power subsystem (PWR) includes the battery and its charger. The passive instrumentation includes plasma wave detectors, an energetic electron analyzer, a photometer, a beam monitor television camera, a Langmuir probe, and a pressure gauge. These subsystems were developed by the Japanese team with support by Toshiba, MELCO, MHI, Meisei Electric Co., and Furukawa Battery Co. The control and data management subsystems include the dedicated experiment processor (DEP), interface unit

(IU), and their control software, and were developed by the U.S. team with support by SWRI and Intermetrics. Table 1 is a summary of the SEPAC instrumentation. Figure 1 shows the components of SEPAC. The SL 1 configuration for SEPAC is shown in Figure 2. SEPAC will be augmented by a plasma contactor (PC) provided by Hughes Research Laboratory through SWRI on ATLAS 1. MPD and NGP will not fly on ATLAS 1. Figures 3 and 4 show the ATLAS 1 configuration.

## 2.1 ACTIVE INSTRUMENTATION

### 2.1.1 Electron Beam Accelerator (EBA)

The EBA is an adjustable output electron gun with beam focusing and deflection. A sketch of the EBA is shown in Figure 5 and a photo in Figure 6. The Pierce-type electron source with a wehnelt electrode can emit an electron beam with an initial diameter of 20 mm and a perveance of  $2.5 \times 10^{-6} \text{ A/V}^{3/2}$ . The cathode of the electron source is a barium impregnated tungsten disk with a diameter of 20 mm and, at a cathode temperature of 1050 C, it can emit a current density of up to about  $5 \times 10^3 \text{ A/m}^2$ . The EBA can emit a beam of electrons with an energy up to 7.5 keV and a current up to 1.6 A (limited by the perveance). Referring to Figure 5, the current emitted by the cathode is limited by the voltage applied between the cathode and the anode ( $V_a$ ). The energy of the beam,  $E_p$ , on the other hand, is determined by the voltage between the body and the cathode ( $V_b$ ), through the relation,  $E_p = eV_b$ , where  $e$  is the charge of an electron. The voltage and current of the beam can thus be set by adjusting  $V_b$  and  $V_a$ , respectively, within

the perveance limits of the cathode. Figure 7 shows the EBA operating region and the beam energy-current combinations available for use on SL 1. On SL 1, the maximum beam energy and current used were 5 keV and 0.3 A, respectively.

Adsorption of contaminants on the surface of the cathode can significantly reduce its emissivity, but it can be reactivated by heating the cathode, diffusing the activating barium to the surface of the cathode. This procedure has the undesirable side effect of significantly reducing its life, however.

The focusing coil is located above the electron gun and is designed to minimize beam spreading by electrostatic forces. The current of the focusing coil was selected after extensive chamber testing to determine the best compromise between beam size and aberration. Above the focusing coil are the four deflection coils. They can deflect the beam up to 30 degrees in any direction off the centerline of the EBA. Software calculates the direction of the Earth's magnetic field with respect to the EBA and can direct the beam so that the beam pitch angle is minimized or in any direction within 30 degrees of the axis.

The EBA and the MPD-AJ (see next section) derive their high voltages from the high voltage converter (HVC). The HVC is a DC-DC converter power supply which uses a supply of 480 V DC power (from the battery, see Section 4.2.3) and has an output up to 7.5 kV at 1.6 A. Power conversion is accomplished with six silicon controlled rectifier based series resonance modules which operate at frequencies between 1 and 10 kHz, depending on the load. The outputs of the modules are isolated from the

inputs and connected in series. This allows operation of the systems even if one or more of the modules fails.

### 2.1.2 Magneto-Plasma Dynamic Arc Jet (MPD-AJ)

The MPD-AJ is a plasma accelerator in which argon is ionized and accelerated by an electrical discharge between coaxial electrodes. It is operated in a pulsed mode, but the pulses are long enough (1 ms) that the discharge maintains itself in a quasi-steady state. Figure 8 shows a sketch of the MPD-AJ (and NGP, which is housed in the same box, see Section 2.1.3), and Figure 9 is a photo of the MPD-AJ/NGP. The MPD-AJ operation results in a cloud of argon plasma with  $10^{19}$  ion pairs and an estimated ion density of  $10^{15}$  to  $10^{17}$   $\text{m}^{-3}$  at 14 m from the MPD-AJ with electron and ion temperatures of 3-5 eV.

The increased plasma density near the orbiter resulting from MPD-AJ operation allows increased return current, which in turn decreases orbiter charging. Operation begins with the venting of a  $3 \times 10^{-5}$   $\text{m}^3$  reservoir of argon at a pressure of 2 or 3 atmospheres by a fast acting (400 microS) valve. After a delay of 1.15 ms, a 15 mF capacitor bank, at a voltage of 400 or 480 volts, is connected to the coaxial electrodes of the MPD-AJ. Delayed by 50 microseconds, a triggering discharge is then created by discharging a 220 microF capacitor at 2 kV to a trigger electrode located close to the center, main electrode. The major discharge lasts for about 1 ms with a current of about 10 kA. This causes the plasma to be blown out of the MPD-AJ with a speed of  $2 \times 10^4$  m/s. The maximum repetition rate of the MPD/AJ is once per 15 s.

### 2.1.3 Neutral Gas Plume (NGP)

The NGP ejects a cloud of nitrogen into the region above the payload bay to provide additional neutral gas near the electron beam. The beam will ionize many of the nitrogen molecules, providing additional return current to the orbiter, reducing its potential.

During operation, cold nitrogen gas is vented to space through a laval nozzle at a pressure of  $10 \text{ kg/cm}^2$  for 0.1 s, releasing about  $10^{23}$  molecules. The laval nozzle is cone-shaped, with a half angle of 15 deg, a throat diameter of 4.05 mm and an exit diameter of 20.23 mm, giving an area expansion ratio of 25. The gas velocity is about 400 m/s, and the density during a shot, 10 m from the nozzle, is about  $1.5 \times 10^{19} \text{ m}^{-3}$ . The estimated distribution of nitrogen near the NGP is shown in Figure 10.

### 2.1.4 Charge Collection Devices (CCD)

On Spacelab 1, the SEPAC instruments detected significant charging of the Shuttle at EBA currents of about 50 mA and charging to the electron beam energy at currents between 50 and 300 mA. Charging at these levels was in the range of preflight predictions based on the known conducting surface area of the Orbiter and Spacelab ( $<100 \text{ m}^2$ ). The conducting areas were primarily the main engine bells, the inner surfaces of the open payload doors, the conductive threads woven into the payload thermal blankets, and the exposed parts of some instruments.

Attempts to further neutralize the shuttle potential during electron beam emission by operating the MPD and the NGP were

only partially successful. In the case of the NGP, secondary electrons produced in the N<sub>2</sub> gas plume by the electron beam represent a potential extra source of neutralizing current. In preflight chamber tests, the neutralizing effect was minimal at low beam currents but stronger at higher beam currents of a few hundred mA. At these higher beam currents, the presence of the neutral gas cloud seemed to produce a discharge effect (perhaps the beam plasma discharge), which actually hindered, rather than aided, escape of an organized beam of electrons. On Spacelab 1 a joint PICPAB/SEPAC experiment investigated the neutralization effects of the NGP for 10 mA beams. In agreement with laboratory experiments, the neutral gas cloud was not effective in neutralizing the rather low (10 V) charging potentials produced by the 10 mA beam.

Neutralization of the orbiter by the MPD plasma cloud was more successful, but for only a very short time. In fact, total charge neutralization was observed during approximately the first 15 mS after beam onset, after which the potential rose to levels similar to the EBA-only beam emissions.

For the ATLAS 1 mission, new means of neutralizing the current ejected by the EBA will be investigated. One approach will be to evaluate the effectiveness of increasing the conductive area of the Orbiter and Spacelab. Another approach will be to use a plasma contactor.

A number of ways to increase the conductive area were considered, including adding more conductive thread to the thermal blankets and using a thermal blanket with an indium oxide conducting coating.

Localized conducting surfaces (charge collection devices, CCD) with direct electrical connections to the Orbiter structure ground will be used. The surface area of these conductors projected on a plane perpendicular to the local magnetic field should be the same for all Orbiter attitudes. A set of three truncated spherical conductors was selected. The spheres will be mounted with their bases parallel to the X, Y plane. With this mounting arrangement, the 1020 mm diameter spheres will increase the conducting area of the Shuttle by about 8%, and they will present very nearly the same cross-sectional area for most attitudes. For thermal reasons, the spheres are painted with a special black paint, which is conducting.

#### 2.1.5 Plasma Contactor

In addition, a plasma contactor will be used on ATLAS 1. It will be a ring-cusp plasma contactor producing a local high density (about  $10^{17} \text{ m}^{-3}$ ) xenon plasma that diffuses into space through the 250 mm diameter exit opening of the contactor. The high electrical conductivity of the plasma prevents the development of significant potential differences between the Orbiter ground and the space plasma, even when amperes of electrons are being actively ejected by the EBA.

The current handling capability of a plasma contactor is equal to the sum of its maximum ion emission current and maximum electron collection current. Both theory [Hastings, 1987, and Parks and Katz, 1987] and ground-simulation experiments [Wilbur, 1986] have indicated that these parameters are related: the maximum electron collection current of a plasma contactor is

predicted to be equal to its ion production current multiplied by a factor which is of order 1 to 10. To assure success, the plasma is designed to produce an ion production current equal to the 1.6 A EBA maximum beam current.

The plasma contactor is a Penning-discharge device, consisting of an anode and cathode with an interposed magnetic field, which serves to restrict electron access to the anode. The anode is a 250 mm diameter hollow iron cylinder that is open to space on the outside end and closed (by an iron plate) on the inside end, i.e., that nearest the Orbiter. Three circumferential rings of rare earth-cobalt magnets are attached to the inner iron surfaces, producing a "ring-cusp" shaped magnetic field that covers the anode surface.

Electrons are released into the contactor from a hollow cathode, centrally located on the inner anode wall. These electrons are accelerated through the 30 V anode to cathode potential drop. Since they are trapped by the magnetic field, the electrons can reach the anode only after experiencing a number of collisions; the 30 V potential difference is chosen to maximize the ratio of ionizing collisions to other types of collisions.

The contactor uses Xenon gas, which is introduced from a storage tank through both the hollow cathode and a gas plenum located on the inner anode wall. More than 90% of this gas is ionized by electron impact in passing through the Penning discharge chamber. The resulting plasma diffuses outward into space, forming an electrically conductive "plasma bridge" to the

ambient space plasma. For discussions of plasma bridge physics, see Hastings [1987] and Parks and Katz [1987]. The contactor can be turned on and off by switching the anode cathode potential; the response times are characteristic of the sonic filling/emptying times of the discharge chamber, i.e., less than 1 mS.

The plasma contactor design is derived directly from ion-propulsion technology resulting in a high gas efficiency and high power efficiency (less than 150 W per ampere of ion current).

The PC will include a neutral gas release, using Xenon, that will release about  $10^{23}$  molecules in 0.1 s. The neutral gas release will be operated independently from the plasma release.

## 2.2 PASSIVE INSTRUMENTATION

SEPAC passive instrumentation is devoted to diagnosing the results of the perturbation of the EBA, MPD-AJ, and NGP on the ambient ionosphere. The passive instrumentation consists of the Diagnostics Package (DGP) and the Monitor Television (MTV).

### 2.2.1 Diagnostics Package (DGP)

The DGP consists of plasma wave instrumentation, an energetic particle analyzer, a vacuum gauge, a photometer, and a Langmuir probe. Figure 11 is a photo of the DGP.

#### 2.2.1.1 Plasma Wave Instruments

Four separate instruments comprise the plasma wave instrumentation. They are the three floating probes (FP), the low-frequency plasma wave probe (PWL), the high-frequency plasma

wave probe (PWH), and the wide-band wave system (WB).

The FP sensors consist of three gold-plated cylinders, 40 mm in diameter and 40 mm in length, mounted 290 mm, 540 mm, and 790 mm above the top surface of the DGP on an insulated rod 25 mm in diameter. Figure 12 shows the configuration. A block diagram of the FP electronics is given in Figure 13. The input impedances of the FP input amplifiers are 10 Megohms. The frequency range of the upper FP is 0 - 400 Hz and for the middle and lower probes, 0 - 200 Hz. The output for the top probe is sampled at a 1 ks/s rate and for the middle and bottom probes, 0.5 ks/s. The mounting location of the sensor cylinders in the payload on SL 1 (see Figure 2) probably meant that they were in the sheath of the orbiter most of the time. A similar situation is expected for ATLAS 1, see Figure 3.

The PWL measures the current to a Faraday cup mounted above the DGP and the potential induced on the outer cylinder of the Faraday cup. The Faraday cup is gold-plated aluminum with an entrance aperture diameter of 40 mm. The outer dimensions of the cup are 70 mm in diameter and 75 mm high. The bottom of the Faraday cup is 435 mm above the DGP upper surface, see Figure 14.

The PWL sensors, the Faraday cup, and the outer surface of the Faraday cup use preamplification with an input impedance of 1 Megaohm and drive two synchronized sweep frequency receivers which measure the intensity of the variations in the sensor signals over the frequency range from 750 Hz to 10 kHz. This range is divided into 255 steps and a complete sweep of the

40 Hz wide bands takes 1 s. Figure 15 gives the block diagram of PWL, PWH, and WB.

Broad band signals with a frequency range of 0.4 to 10 kHz from the Faraday cup body pass through an automatic gain control (AGC) amplifier with a 75 dB range and are passed to the Wide Band (WB) system described below.

The PWH sensor is the 30 mm diameter by 435 mm long gold-plated aluminum cylinder that supports the PWL Faraday cup and which is mounted to the top of the DGP. Figure 14 shows the PWH sensor and Figure 15, the PWH electronics. After preamplification, the PWH signal drives a sweep frequency receiver. The sweep frequency receiver covers the range from 0.1 to 10.5 MHz, with 2046 steps, each step having a bandwidth of 10 kHz and a frequency separation of 4 kHz. The intensity of the received waves is measured once per ms so that a complete sweep takes 2 s. The receiver can also continuously measure the wave intensity at any of the 2046 frequency steps. The measurement range is from  $2 \times 10^{-7}$  to  $10^{-1}$  volts. Broad band signals in frequency ranges from 0.1 to 4.2 MHz or 4.0 to 7.5 MHz (frequency shifted to 0 to 3.5 MHz in the case of the upper frequency range) pass through an AGC receiver with a range of 75 dB, and then are sent to the WB system.

The WB system combines the outputs of the AGC receivers in the PWL and PWH. Spacelab then sends the composite analog signal to the Shuttle for transmission to the ground via an analog data channel. Figure 15 also shows the block diagram of WB.

### 2.2.1.2 Energetic Particle Analyzer-Electron (EPA-E)

The EPA-E is a hemispherical electrostatic energy analyzer (gold-plated aluminum) with four detectors, a channeltron, and three Faraday cups. A sketch of the EPA-E analyzer and electronic block diagram is shown in Figure 16. The instrument measures electron fluxes at 32 energies from 0.1 to 15 keV with an approximate energy resolution of + or - 18%.

The field of view of the analyzer is  $4 \times 10$  deg, with the viewing angle pointed out of the payload bay, in the -Z direction. Fluxes from  $2 \times 10^6$  to  $1 \times 10^{10}$   $(\text{cm}^2 \cdot \text{s} \cdot \text{ster} \cdot \text{keV})^{-1}$  for the channeltron and from  $1 \times 10^{-10}$  to  $2 \times 10^{-4}$  A/cm<sup>2</sup> for the Faraday cup can be measured with EPA-E. The channeltron data register is open for 1 ms and read out every 1 ms. Two of the Faraday cup currents are sampled every 1 ms (or 125 microseconds during burst mode). The third Faraday cup is sampled every 4 ms.

During the Spacelab 1 mission, the EPA-E measured the energy spectrum of the electrons returning to the Orbiter during EBA operations. These spectra showed that the vehicle charged to the beam potential at the higher current levels. However, the channeltron detector exhibited an afterpulse phenomenon which resulted in a period of false counts following the termination of beam current. This phenomenon may have resulted from outgassing within the detector at the elevated gas pressures within the payload bay or from a defective channeltron. Necessary repairs will be made for the ATLAS 1 mission.

In addition, at high input fluxes, the analog pulse heights

were below the design level, leading to an apparent lower count rate than expected. Reduction of the aperture size and changing the discrimination level of the triggering circuit will solve this problem for ATLAS 1.

#### 2.2.1.3 Energetic Particle Analyzer-Vacuum (EPA-V)

The EPA-V is a nude ionization gauge with two (redundant) filaments. (It was specially designed and made by Nihon Sinku.) The filaments emit electrons which are accelerated to 150 volts to ionize the neutral gases in the gauge. The resulting ions are then accelerated, and their current to a collector is measured. The ion current is proportional to the ambient pressure. The range of measurable pressures is  $5 \times 10^{-8}$  to  $5 \times 10^{-4}$  torr, for an  $N_2$  atmosphere. Its accuracy is better than 20%. Reported SEPAC pressures are referenced to molecular nitrogen. The ambient atmospheric composition at the altitude of SL 1 and ATLAS 1 (250 km) is 55-95% atomic oxygen with virtually all the rest being molecular nitrogen (NOAA, et al., 1976).

#### 2.2.1.4 Photometer (PHO)

The PHO is a gimballed optical system with a photomultiplier (Hamamatsu Photonics R376) sensor to detect natural and artificial optical emissions. The one axis gimbal is about the X-axis and has 120 deg of motion centered on the -Z-axis, see Figure 2. The 90 mm objective lens is followed by a filter wheel with three interference filters at 3914, 5577, and 6300A and a standard light source for calibration. The filter wheel

is followed by an iris at the focal plane to limit the field of view (0 to 8.8 deg) and to limit the intensity of the light on the photomultiplier tube. The photomultiplier current is measured every 1 ms.

#### 2.2.1.5 Langmuir Probe (LP)

The LP is a traditional cylindrical plasma probe operated with fixed and swept bias, utilized to measure thermal electron parameters.

The sensor is a gold-plated, stainless steel cylinder, 4 mm in diameter and 200 mm long. A guard electrode, 8 mm in diameter and 150 mm long is placed below and separated from the sensor by a small supporting insulator. The guard and probe are mounted on a 250 mm long supporting insulator on the top of the DGP. Figure 17 is a sketch of the LP sensor. Either a sweeping voltage (sawtooth, -9 V to +9 V in 84 ms) or a fixed voltage (0, +3, +6, or +9 V) is applied to the probe and guard electrodes, and the current and voltage to the probe are measured every 1 ms and 4 ms, respectively. The LP was chemically cleaned prior to launch, but no probe cleaning was performed during the SL 1 mission. The block diagram of the LP electronics is shown in Figure 18.

Using the voltage and current measurements, the electron density and temperature of the plasma at the LP can be determined. In addition, the LP can measure the vehicle potential with respect to the plasma potential at the LP if that potential is between -9 and +9 V.

### 2.3 Monitor Television (MTV)

The MTV is a two axis gimballed television camera for imaging the light from the interactions of the electrons, plasma, and atmosphere near Spacelab. Figure 19 shows a photograph of the MTV.

The pointing system has an elevation range of -30 to +120 degrees and an azimuth range of -90 to +90 degrees.

The MTV is in a canister with a glass window of VYCOR-CODE #7913 which has a transmittance of 90% in the visible. It uses a 25 mm focal length lens with an F ratio of 0.81. The imaging tube is a 16 mm silicon intensified target vidicon (RCA 4804), giving a field of view of 28.7 by 21.7 deg. Its focus is fixed at 13 m. The spectral response is from 390 to 700 nm (peaked at 450 nm) and has a sensitivity limit of  $6 \times 10^{-4}$  lux (with a standard tungsten light source). The video signal is a standard (NTSC) monochrome television signal and is sent to the ground on the TV channel. The resolution of the image from the MTV depends on the source brightness, see Figure 20.

### 2.4 SUPPORT HARDWARE

#### 2.4.1 Interface Unit (IU)

The interface unit (IU) is that system which forms the electrical and logical interface between the SEPAC instrumentation and Spacelab. The IU is an intelligent input/out (I/O) device for the Dedicated Experiment Processor (DEP). The IU interfaces with the DEP, the SEPAC instrumentation and the Spacelab data acquisition and control systems. The IU performs the function of data acquisition,

instrumentation commanding (when instructed to do so by the DEP), Spacelab communications, communications with other instruments, and timekeeping.

#### 2.4.1.1 Data Acquisition

The IU acquires analog and digital data from the instrumentation using a hybridized telemetry encoder with several pre-encoders. The IU encodes the data into a single 512 kbps composite data stream. Table 2 summarizes the total telemetry data acquisition capability for the IU. A complete summary of the SEPAC data is given in Yanagisawa, et al. (1985).

The IU features a very high speed analog data acquisition subsystem called the burst mode logic (BML), designed specifically to monitor critical beam firing parameters and to transfer these data directly into DEP memory using a direct memory access (DMA) channel. The BML subsystem acquires 250 samples from each of 32 EBA data channels in 31 milliseconds and 4 MPD channels in 4 milliseconds. The start of BML data acquisition begins with the IU master 1 Hz timing signal. Having acquired the data, the BML then stores the data in the DEP (see Section 2.4.2.2) and later forwards it at a reduced rate to the IU telemetry data encoder. Engineering data, including instrumentation commands, status words, and housekeeping data, are also monitored and inserted into the 512 kbps data stream.

#### 2.4.1.2 Instrumentation Commanding

The role of the IU in instrumentation commanding is to receive command instructions from the DEP and to convert these

instructions into analog or discrete signals compatible with instrumentation interfaces. Table 3 summarizes the IU command capability.

The MTV presents a special case for instrument commanding since it may be controlled manually by the Spacelab crew or automatically under DEP software control. This functionality is achieved through the use of analog switches which gate control signals through to the MTV from either the DEP or SEPAC control panel depending on the state of the "auto/manual" switch on the control panel.

#### 2.4.1.3 Spacelab Communications

Communications with the Spacelab Experiment Computer (EC) is accomplished within the IU with a microprocessor controller communications subsystem called the link manager (LM). Messages for the EC originating from SEPAC or vice versa are passed by the DEP to the LM through the dual ported memory. When communications errors develop, it is the responsibility of the LM to recover. Under extreme conditions, the LM will clear all message available flags and interrupt the DEP with a request to retransmit its last message. The IU/EC communications link uses a one Mbps data rate with a maximum message length of 32 sixteen bit words.

#### 2.4.1.4 Communications with Other Instruments

To coordinate SL 1 experiments and to protect their instrumentation, SEPAC, AEPI, and PICPAB communicated with each other directly. For SEPAC, this was accomplished in the IU. The IU can generate eight differential discrete output signals

and receive eight discrete signals from other sources through electrically isolating optical couplers. For SL 1, two output and two input signals were actually connected to other instruments. One output was sent to AEPI to turn their video camera high voltage off during EBA operations. An input from AEPI was used as a signal to SEPAC software to proceed with FO execution for joint SEPAC/AEPI operations. The second output bit was routed to PICPAB and denoted EBA firing. The second input bit came from PICPAB and signaled its electron accelerator firing.

#### 2.4.1.5 Timekeeping

In order for the SEPAC DEP to properly time the events during a functional objective, the IU includes a real time GMT clock. This clock communicates with the LM, DEP, and high rate multiplexer (HRM is a Spacelab subsystem). Time is initially preset by the LM based on a GMT message from the EC. The GMT clock is updated by the 1024 kHz clock signal from the EC. The GMT clock provides day of the year, milliseconds of the day, and 1/256's of milliseconds.

#### 2.4.2 Dedicated Experiment Processor (DEP)

For SL 1, SEPAC used a NASA standard spacecraft computer, Version II (NSSC II, not related to the NSSC I) as the dedicated experiment computer (DEP). The NSSC II is a microprogram controlled, general purpose, 16 bit, parallel computer with 64K bytes of user available memory. It has a dedicated direct memory access channel, direct and buffered I/O ports and maskable interrupts. For future missions, use of an SWRI SC-1

computer is planned. The DEP is used for calculations and for controlling I/O. Figure 21 is a block diagram of the SEPAC command and data management system (CDMS) showing the relationship between the DEP and the IU. The DEP interfaces only with the IU.

#### 2.4.2.1 Memory Loads

The NSSC II had no non-volatile memory, so its memory had to be reloaded each time power was applied to the computer. This was done using either IU logic and memory (primary load) or the Spacelab mass memory unit (MMU) and EC, in conjunction with the communications controller of the IU (backup load).

In normal operations (primary load), the IU LM reloaded the memory of the NSSC II each time power was turned on, using the direct I/O interface channel of the NSSC II. Since the NSSC II was designed to be loaded from a magnetic tape drive, the IU was equipped with a tape drive hardware emulator. As power was applied, the IU converted the NSSC II operation codes stored in IU memory into initial program load (IPL) format and passed formatted operation codes to the computer one byte at a time. The primary load process took about 35 seconds to complete.

A backup load was initiated by the EC. After receiving a backup load message from the EC, the LM used an NSSC II control interrupt to halt program execution and to place a small loader program into NSSC II memory. This loader program ran throughout the transmission of the several hundred data blocks from the EC and MMU. For each new data block received, the LM and the DEP independently calculated the checksum of the block and compared

results. If the results matched, the new block was stored in computer memory. If not, the LM requested retransmission of the block from the EC and MMU. Likewise, as each new block was received, the LM and NSSC II independently verified the sequence number of the block. In the event of a block sequence error, the IU terminated the load and notified the EC. A backup load took a minimum of 4.5 minutes.

#### 2.4.2.2 Communications

The NSSC II communicated with the SEPAC instrumentation by using its direct I/O channel to send commands through the IU to the instrumentation. Thus, the IU functioned as an intelligent input/output processor to support NSSC II operations. The DMA of the USSC II was used for storing digitized analog signals acquired by the BML during EBA and MPD-AJ firings. This dedicated the DMA channel to acquiring science data and therefore was not used during initial program loading. The NSSC II also sent status messages in the data stream, including software status, communications status, some messages from Spacelab, and error flags.

#### 2.4.2.3 Performance

Throughout the development of the SEPAC CDMS for SL 1, problems were experienced with the NSSC II I/O channel handshaking logic. The cause was inadequate noise immunity. These handshaking logic problems caused the computer to stop running completely. The NSSC II stopped four times during the SL 1 mission.

#### 2.4.3 Power System (PWR)

The power subsystem (PWR) consists of the energy storing battery and its charger. It is used to provide high electrical power for the HVC, which provides high voltage for the EBA and MPD-AJ. Using PWR reduces the high power required by SEPAC, but the energy requirements are somewhat increased due to the battery charge/discharge losses. The battery has 320 NiCd cells connected in series; each cell is rated at 4.0 AH. The battery is divided into sets of 32 cells with the voltage of each set monitored separately. The charger converts 28 V DC Spacelab power to a current controlled voltage in the 200-480 V range for battery charging.

#### 2.4.4 Control Panel (CP)

The control panel (CP) mounts in either a standard Spacelab rack or in the aft flight deck of the orbiter. It is used by the payload crew to control the power systems and the MTV of SEPAC. A line drawing of the CP is shown in Figure 22. The MTV section of the CP includes iris, electronic sensitivity and gain, and gimbal controls.

### 3.0 SOFTWARE

SEPAC DEP software implemented the command and control functions necessary to perform SEPAC operations. The NSSC II emulated an extended version of the IBM 360 instruction set. The software was written in IBM FORTRAN H and assembly language and used a System 360 as host computer. The software provided experiment sequencing, Spacelab/crew interfacing, contingency

operations, and status reporting. These topics are discussed in the following sections.

### 3.1 FO Sequencing

NSSC II software scheduled up to four functional objectives (FOs) during each period of operation. FOs were initiated at the proper times by monitoring the GMT clock maintained by the IU. FOs were performed by executing encoded tables of commands. Tables for 18 different FOs were available in the MMU. Most SEPAC FOs were divided into five distinct phases as follows:

1. Parameter Change File (PCF) update
2. FO preparation
3. System (or SEPAC) manual operation (SMO)
4. Automatic experiment operations
5. Shutdown

#### 3.1.1 Parameter Change File Update

Most FOs included a PCF which contained various default instrument settings for the FO. Using SEPAC EC Applications Software (ECAS), it was possible to alter these settings. Examples include EBA beam current, and MTV iris size. Each PCF was further divided into parameters which took effect during SMO and those which were used for automatic experiment operations. When PCF updates were completed, the crew commanded the software to proceed to the next phase, which was FO Preparation (FO PREP).

### 3.1.2 FO Preparation

During the FO PREP phase, power was applied to instrumentation, and it was configured for SMO or automatic experiment operations. FO PREP was completely controlled by DEP software and proceeded automatically until time to commence the next experiment phase. The crew was notified when FO PREP was complete by a message from the DEP.

The time allocated for FO PREP varied, depending upon the time between FOs. Nominal duration for the first FO in a sequence of FOs was eight minutes, most of which was dedicated to warming up the EBA cathode. If the cathode was already warm from previous FOs, the FO PREP time for subsequent FOs was reduced.

### 3.1.3 System (or SEPAC) Manual Operation

SMO allowed the EBA to be fired at varying frequencies, power levels, and durations under crew control. SMO was an optional phase selected by PCF update. The crew was notified by a message from the DEP when SMO operations were allowed, and they could alter beam firing parameters between individual firings. SMO operations were nominally allocated two minutes and were terminated by crew command. Following SMO, automatic experiment commands were initiated at the FO schedule time.

### 3.1.4 Automatic Experiment Operation

During the automatic experiment operation phase of an FO, SEPAC instrumentation was commanded by the software command tables. It was possible to suspend and restart automatic operations via crew command. During suspended periods, PCF

updates were allowed and took effect when operation was restarted (at T=0, the beginning of the automatic experiment operation). Commands to individual instruments were transmitted every 100 msec and synchronized with the master 1 Hz timing signal from the IU.

### 3.1.5 Shutdown

When automatic experiment operations were completed, instrumentation shutdown was initiated. Depending upon the number of FOs remaining and the time between them, the shutdown sequence completely shut the instrumentation down or placed some instruments in a stand-by state. This reduced the time required for FO PREP for the next FO. The crew was notified when shutdown was complete, and the next FO was then scheduled. PCF updates and remaining phases for that FO could then be performed.

## 3.2 Spacelab/Crew Interface

SEPAC operations were supported by three crew display pages provided by the EC Operating System (ECOS) and ECAS and were displayed on the Spacelab Digital Display Unit (DDU). One page displayed the status of SEPAC instrumentation and systems. This page was completely maintained by ECOS and was available to the payload crew at all times. Two additional display pages were provided by ECAS whenever SEPAC was operating. SEPAC ECAS also accepted crew commands and displayed SEPAC status on the DDU. Two display pages were maintained by ECAS, one of which was dedicated to SEPAC control and the other to graphic display of SEPAC scientific data. Control functions available to the crew

included:

- o PCF update
- o SMO operations
- o Manual instrument shutdown
- o FO hold/restart
- o Automatic shutdown enable/inhibit

These operations were requested by the crew from the Spacelab Keyboard (KB), transmitted by ECAS to the IU, and subsequently relayed to the DEP for implementation. SEPAC DEP software returned the results of any crew input to ECAS for display.

During automatic experiment operations, data gathered by the IU BML subsystem for EBA and MPD firings were passed to the DEP by direct memory access (DMA). These data were processed, formatted, and transmitted to the EC for graphic display by SEPAC ECAS on the DDU.

In addition to crew interface, ECOS provided SEPAC with exception monitoring (checking to see if parameters out of specified limits) services during experiment operations. These were reported to the crew and if serious, ECOS signaled the DEP to turn off instrumentation.

### 3.3 Contingency Operations

SEPAC flight software provided for contingency operations in the event of partial or complete failure of SEPAC instruments. These contingency modes could be invoked automatically or in response to crew command. Automatic shutdown commands issued by ECOS or ECAS in response to out-of-limit conditions allowed the

NSSDC II to power-down individual instruments without aborting an entire FO. Additionally, the PCF contained entries to invoke redundant hardware or alternate operating modes for certain instruments.

Also included were facilities to allow ground test and checkout of instruments.

### 3.4 Status Reporting

The IU contained 512 bytes of dual ported memory which was downlinked in SEPAC's telemetry stream once per second. SEPAC software placed status information in this memory indicating the current operating configuration of SEPAC and the health of the CDMS system. Included in this information were:

- o Current magnetic field data from a model in the EC
- o Software status
- o Experiment operating mode
- o Last IU/DEP message transaction
- o Current Guidance, Navigation, and Control (GN&C) data
- o Error flags

### 4.0 IN FLIGHT OPERATIONS

During the SL 1 mission, SEPAC instrumentation operated flawlessly, with two exceptions: the cathode heater power supply of the EBA and the on board burst mode graphics display. The cathode heater power supply failed during the fourth day of the mission, limiting further active experiments to stimulation by the MPD, NGP, or the PICPAB instrumentation. The burst mode graphics display appears to have failed during ground testing

and was not available for any of the SL 1 flight. Several Spacelab problems affected SEPAC as well. The most serious was the intermittent inoperability of the Remote Acquisition Unit (RAU), which was the interface between the SEPAC DEP and the Spacelab Experiment Computer.

Nevertheless, 28 scientific Functional Objectives (periods of experimental operations) were performed using all of the SEPAC equipment. Approximately  $10^{10}$  bits of direct digital data,  $4 \times 10^{11}$  bits of analog data (equivalent) and  $3 \times 10^{11}$  bits of television data (equivalent) were collected for analysis by SEPAC during the SL 1 mission. The SEPAC experiments (in terms of FOs) performed during the SL 1 mission are listed in Table 4.

## BIBLIOGRAPHY

- Obayashi, T., N. Kawashima, K. Kuriki, N. Nagatomo, K. Ninomiya  
S. Sasaki, A. Ushirokawa, I. Kudo, M. Ejiri, W. Roberts  
R. Chappell, J. Burch, and P. Banks, Space experiments with  
particle accelerators (SEPAC), Artificial Particle Beams in  
Space Plasma Studies, edited by B. Grandal, NATO Adv. Study  
Inst. Ser., Ser. B, 79, 659-671, 1982.
- Sasaki, S., N. Kawashima, K. Kuriki, M. Yanagisawa, T. Obayashi,  
M. Nagatomo, K. Ninomiya, M. Ejiri, I. Kudo, W.T. Roberts,  
C.R. Chappell, D.L. Reasoner, J.L. Burch, W.W.L. Taylor,  
P.M. Banks, P.R. Williamson, and O.K. Garriott, Gas  
Ionization Phenomena in SEPAC SPACELAB-1 Experiment, ISAS  
Research Note 259, Toyko, Japan, May 1984.
- Sasaki, S., N. Kawashima, K. Kuriki, M. Yanagisawa, T. Obayashi  
M. Nagatomo, K. Ninomiya, M. Ejiri, I. Kudo, W.T. Roberts,  
C.R. Chappell, D.L. Reasoner, J.L. Burch, W.W.L. Taylor,  
P.M. Banks, P.R. Williamson, and O.K. Garriott, Charge  
Build-up of Orbiter Measured in SEPAC SPACELAB-1  
Experiment, ISAS Research Note 260, Tokyo, Japan, May 1984.
- Sasaki, S., N. Kawashima, K. Kuriki, M. Yanagisawa, T. Obayashi,  
M. Nagatomo, K. Ninomiya, M. Ejiri, I. Kudo, W.T. Roberts,  
C.R. Chappell, D.L. Reasoner, J.L. Burch, W.W.L. Taylor,  
P.M. Banks, P.R. Williamson, and O.K. Garriott,  
Neutralization Effect of a Plasma and Gas Plume on the  
Charging of Orbiter in SEPAC Spacelab-1 Experiment, ISAS  
Research Note 262, Tokyo, Japan, 1984.

Sasaki, S., N. Kawashima, K. Kuriki, M. Yanagisawa, T. Obayashi, M. Nagatomo, K. Ninomiya, M. Ejiri, I. Kudo, W.T. Roberts, C.R. Chappell, D.L. Reasoner, J.L. Burch, W.W.L. Taylor, P.M. Banks, P.R. Williamson, and O.K. Garriott, Verification of the Critical Velocity Ionization in SEPAC Spacelab-1 Experiment, ISAS Research Note 265, Tokyo, Japan, June 1984.

Obayashi, T., N. Kawashima, K. Kuriki, M. Nagatomo, K. Ninomiya, S. Sasaki, M. Yanagisawa, I. Kudo, M. Ejiri, W.T. Roberts, C.R. Chappell, D.L. Reasoner, J.L. Burch, W.W.L. Taylor, P.M. Banks, P.R. Williamson, and O.K. Garriott, Space Experiments with Particle Accelerators, Science, 225, 195-196, 1984.

SEPAC Science Report 5 (Sasaki, please add)

Sasaki, S., S. Kubota, N. Kawashima, K. Kuriki, M. Yanagisawa, and T. Obayashi, Ignition of Beam Plasma Discharge Observed in Spacelab-1 SEPAC/PICPAB Joint Experiment, ISAS Research Note 269, Tokyo, Japan, September 1984.

Yanagisawa, M., S. Sasaki, N. Kawashima, and T. Obayashi, SEPAC Data Base Product Tape, ISAS Research Note 283, Tokyo, Japan, March 1985.

Akai, K., Electron Beam - Plasma Interaction Experiment in Space, ISAS Research Note 285, Tokyo, Japan, April 1985.

Taylor, W.W.L., T. Obayashi, N. Kawashima, S. Sasaki, M. Yanagisawa, J.L. Burch, D.L. Reasoner, and W.T. Roberts, Wave-particle interactions induced by SEPAC on Spacelab 1: Wave observations, Rad. Sci., 20, 486-498, 1985.

- Cai, D., S. Sasaki, and K. Abe, Extremely Low Frequency Oscillations Excited by Electron Beam Injection in SEPAC Spacelab-1 Experiment, ISAS Research Note 298, Tokyo, Japan, September 1985.
- Sasaki, S., N. Kawashima, K. Kuriki, M. Yanagisawa, T. Obayashi, W.T. Roberts, D.L. Reasoner, W.W.L. Taylor, P.R. Williamson, P.M. Banks, and J.L. Burch, Ignition of Beam Plasma Discharge in the Electron Beam Experiment in Space, Geophys. Res. Lett., 12, 647-650, 1985.
- Sasaki, S., N. Kawashima, K. Kuriki, M. Yanagisawa, and T. Obayashi, Vehicle Charging Observed in SEPAC Spacelab-1 Experiment, J. of Spacec. and Roc., 23, 194-199, 1986.
- Sasaki, S., N. Kawashima, K. Kuriki, M. Yanagisawa, T. Obayashi, W.T. Roberts, D.L. Reasoner, W.W.L. Taylor P.R. Williamson, P.M. Banks, and J.L. Burch, Gas ionization induced by a high speed plasma injection in space, Geophys. Res. Lett., 23, 434, 1986.
- Burch, J.L., Space Plasma Physics Results from Spacelab 1, J. of Spacec. and Roc., 23, 331-335, 1986.
- Neubert, T., W.W.L. Taylor, L.R.O. Storey, N. Kawashima, W.T. Roberts, D.L. Reasoner, P.M. Banks, D.A. Gurnett, R.L. Williams, and J.L. Burch, Waves Generated During Electron Beam Emissions from the Space Shuttle, J. of Geophys. Res., 91, 11,321-11,329, 1986.
- Marshall, J.A., C.S. Lin, J.L. Burch, T. Obayashi, and C. Beghin, Spacelab 1 Experiments of Interactions of an Energetic Electron Beam with Neutral Gas, submitted to J. of Spacec. and Roc., 1986.

Cai, D., T. Neubert, L.R.O. Storey, P.M. Banks, S. Sasaki,  
K. Abe, and J.L. Burch, ELF Oscillations Associated with  
Electron Beam Injections from the Space Shuttle, J. of  
Geophys. Res., 91, 12,451-12,457, 1987.

## Table Captions

TABLE 1 SEPAC Instrumentation Summary

TABLE 2 IU Data Acquisition Capability

TABLE 3 IU Command Capability

TABLE 4 SEPAC Experiments During SL 1

## Figure Captions

- Figure 1 Major components of the SEPAC instrumentation: EBA, MPD-AJ, NGP, DGP, MTV, and CCD.
- Figure 2 Placement of the instrumentation on the SL-1 pallet
- Figure 3 Placement of the ATLAS 1 pallets on the Shuttle
- Figure 4 Placement of the instrumentation on the ATLAS 1 pallet
- Figure 5 EBA sketch
- Figure 6 Photo of EBA
- Figure 7 EBA accessible region and operating points
- Figure 8 MPD-AJ sketch. The MPD-AJ uses a copper anode and a tungsten cathode. The separating insulator is coated with boron nitride.
- Figure 9 MPD-AJ photo
- Figure 10 Calculated nitrogen density near the NGP
- Figure 11 Photo of DGP
- Figure 12 Sketch of FP sensors
- Figure 13 FP electronics block diagram
- Figure 14 Faraday Cup (PWL sensors) and PWH sensor
- Figure 15 PWL, PWH, and WB block diagram
- Figure 16 EPA-E sketch and electronic block diagram
- Figure 17 LP sensor sketch
- Figure 18 LP electronics
- Figure 19 MTV photo
- Figure 20 MTV resolution
- Figure 21 CDMS Block Diagram
- Figure 22 Line Drawing of the Control Panel

TABLE 1

Electron Beam Accelerator (EBA, provided by ISAS)

<u>Parameter</u>	<u>Value</u>
Energy	0 to 7.5 keV
Current	0 to 1.6A
Perveance	$2.5 \times 10^{-6} \text{ A/V}^{3/2}$
Initial beam diameter	20 mm
Deflection	$30^\circ$ from axis
Modulation	5 kHz and below

Magnetoplasma Dynamic Arc Jet (MPD-AJ, provided by ISAS)

<u>Parameter</u>	<u>Value</u>
Gas	Argon
Pulse width	1 ms
Energy	2 kJ/pulse
Number of ion-electron pairs	$10^{19}$
Density at 14 m from MPD-AJ outlet	$10^{15}$ to $17 \times 10^{-3} \text{ cm}^{-3}$
Plasma flow speed	$2 \times 10^4 \text{ m/s}$
Temperature of plasma	$T_e = T_i = 3 \times 10^4$ to $5 \times 10^4 \text{ K}$

TABLE 1 (Continued)

Neutral Gas Plume (NGP, provided by ISAS)

<u>Parameter</u>	<u>Value</u>
Gas	Nitrogen
Pulse width	100 ms
Ejection speed	400 m/s
Number of ejected molecules	$10^{23}$
Density at 10 m from NGP outlet	$1.5 \times 10^{19} \text{ m}^{-3}$

Plasma Wave Detectors (provided by ISAS)

<u>Parameter</u>	<u>Value</u>
Floating probes (FP)	3
Frequency range	0 to 400 Hz
Measurement range	-8 kV to +8 kV
Resolution	31 V
Low-frequency plasma wave probes (PWL)	2
Frequency range	0.75 to 10 kHz
Measurement range	
Voltage to FC body	$10^{-4}$ to $7 \times 10^{-1}$ V
Current to FC body	$2.5 \times 10^{-11}$ to $10^{-6}$ A
High-frequency plasma wave probe (PWH)	1
Frequency range	0.1 to 10.5 MHz
Measurement range	$2 \times 10^{-7}$ to $10^{-1}$ V
Receiver type	Stepping
Wide band plasma wave probe (WB)	
Frequency range	0.4 to 10 kHz and 0.1 to 4.2 MHz or 4.0 to 7.5 MHz

TABLE 1 (Continued)

Energetic Electron Analyzer (EPA-E, provided by ISAS)

<u>Parameter</u>	<u>Value</u>
Energy range	0.1 to 15 keV
Flux range	$2 \times 10^6$ to $10^{10}$ ele/cm <sup>2</sup> s st keV (channeltron detector) and $10^{-10}$ to $2 \times 10^{-4}$ A/cm <sup>2</sup> (current collector)
Energy resolution	+ or - 0.18
Entrance Aperture	4° x 10°
Modes	
Fixed energy	100 measurements/s
Energy scan	320 ms/scan

Photometer (PHO, provided by ISAS)

<u>Parameter</u>	<u>Value</u>
Objective lens diameter	90 mm
Measurement ranges and filter widths	
Filter wavelength, nm	Range (Rayleigh)      Width Minimum    Maximum    (FWHM, nm)
391.4	$1.7 \times 10^3$ $7.9 \times 10^8$ 10
557.7	$6.8 \times 10^2$ $1.3 \times 10^8$ 2.5
630.0	$3.1 \times 10^3$ $1.4 \times 10^9$ 2.5
Field of view	0° to 8.8° diameter
Pointing	One axis, 60° from axis
Sampling rate	1 kS/s

TABLE 1 (Continued)

Monitor Television (MTV, provided by ISAS)

<u>Parameter</u>	<u>Value</u>
Type	Monochrome vidicon
Field of view	28.7° by 21.7°
Sensitivity	10 <sup>-2</sup> to 10 <sup>5</sup> lux
Spectral range	3900 Å to 7000 Å
Frame rate	30 Hz

Langmuir Probe (LP, provided by ISAS)

<u>Parameter</u>	<u>Value</u>
Probe size	200 mm long by 4 mm diameter
Current range	10 <sup>-7</sup> to 10 <sup>-4</sup> A
Sampling rate	
Current	1 kS/s
Voltage	250 S/s

Pressure Gauge (EPE-V, provided by ISAS)

<u>Parameter</u>	<u>Value</u>
Type	Ionization gauge
Vacuum range	5 x 10 <sup>-8</sup> to 5 x 10 <sup>-4</sup> torr
Sampling rate	1 kS/s

Support Equipment: Interface unit (IU, provided by SWRI), dedicated experiment processor (DEP, provided by MSFC), high-voltage convertor (HVC, provided by ISAS), power supplies (PS, provided by ISAS), and control panel (CP, provided by ISAS).

TABLE 2

## SEPAC IU Data Acquisition Capability

<u>Description</u>	<u>Number of Channels</u>	<u>Sampling Rate</u> (samples/sec)
Analog (-5 to +5 v)	21	1000
Analog (-5 to +5 v)	5	500
Analog (-5 to +5 v)	57	250
Analog (-5 to +5 v)	96	2
Digital (16 bits)	35	8750
Digital (8 bits)	2	4750
Digital (8 bits)	3	1000
Digital (8 bits)	4	500
Digital (8 bits)	2	250
Digital (8 bits)	4	2

TABLE 3

## SEPAC IU Command Capability

<u>Command Type</u>	<u>Number of Commands Available</u>
Discrete (Single ended)	118
Discrete (True differential)	8
Analog (Single ended)	10

TABLE 4

## SEPAC Experiments Performed on SL 1

<u>Type of Experiment</u>	<u>Number of Functional Objectives</u>
Electron Beam Injection	2
Plasma Injection	8
Simultaneous Electron Beam and Plasma Injection	2
Neutral Gas Injection	2
PICPAB Electron Beam Injection	2
Simultaneous PICPAB and Plasma Injection	4
Simultaneous PICPAB and Neutral Gas Injection	2
Passive Observations	6

## Acknowledgements

SPAN was used in the performance of this research. This work was supported by NASA (U.S. team members) and by the Ministry of Education, Culture, and Science (Japanese team members).

## REFERENCES

- Annales de Geophysique, Special issue on the results of the active French-Soviet Araks experiments, 36, 271-445, 1980.
- Banks, P.M., W.J. Raitt, P.R. Williamson, A.B. White, and R.I. Bush, Results from the Vehicle Charging and Potential Experiment on STS-3, J. of Spacecraft and Rockets, 24, 138-149, 1987.
- Beghin, C., J.P. Lebreton, B.N. Maehlum, J. Troim, P. Ingsoy, and J.L. Michau, Phenomena induced by charged particle beams, Science, 225, 188-191, 1984.
- Grandal, B. (Ed.), Artificial Particle Beams in Space Plasma Studies, NATO Adv. Study Inst. Ser., Series B: Physics, 79, 1982.
- Hastings, D.E., Theory of Plasma Contactors Used in the Ionosphere, J. of Spacecraft and Rockets, 24, 250-256, 1987.
- Israelson, G.A. and J.R. Winckler, Effect of a neutral cloud on the electrical charging of an electron beam-emitting rocket in the ionosphere: Echo IV, J. Geophys. Res., 84, 1442-1452, 1979.
- Mende, S., G.R. Swenson, and K.S. Clifton, Atmospheric Emissions Photometric Imaging Experiment, Science, 225, 191-193, 1984.
- Meriwether, J.W., J.P. Heppner, J.D. Stolarik, and E.M. Wescott, Neutral winds above 200 km at high latitudes, J. Geophys. Res., 78, 6643-6661, 1973.
- National Oceanic and Atmospheric Administration, National Aeronautics and Space Administration, and United States Air Force, U.S. Standard Atmosphere, 1976, Washington, D.C., 1976.

- Obayashi, T., N. Kawashima, K. Kuriki, M. Nagatomo, K. Ninomiya, S. Sasaki, M. Yanagisawa, I. Kudo, M. Ejiri, W.T. Roberts, C.R. Chappell, D.L. Reasoner, J.L. Burch, W.W.L. Taylor, P.M. Banks, P.R. Williamson, and O.K. Garriott, Space experiments with particle accelerators, Science, 225, 195-196, 1984.
- Parks, D.E. and I. Katz, Theory of Plasma Contactors for Electrodynamic Tethered Satellite Systems, J. of Spacecraft and Rockets, 24, 245-249, 1987.
- Radio Science, Special issue on emissions from particle beams in space, 19, 453-586, 1984.
- Shawhan, S.D., G.B. Murphy, P.M. Banks, P.R. Williamson, and W.J. Raitt, Wave emissions from DC and modulated electron beams on STS 3, Radio Sci., 19, 471-486, 1984.
- Taylor, W.W.L., T. Obayashi, N. Kawashima, S. Sasaki, M. Yanagisawa, J.L. Burch, D.L. Reasoner, and W.T. Roberts, Wave-particle interactions induced by SEPAC on Spacelab 1: Wave Observations, Radio Science, 20, 486-498, 1985.
- Wilbur, P.J., Hollow Cathode Plasma Coupling Study, Annual Report, NASA CR 171985, 1986.
- Wilhelm, K., W. Stuedmann, and W. Riedler, Electron flux intensity distributions observed in response to particle beam emissions, Science, 225, 186-188, 1984.
- Winckler, J.R., The application of artificial electron beams to magnetospheric research, Rev. Geophys., 18, 659-682, 1980.
- Yanagisawa, M., S. Sasaki, N. Kawashima, and T. Obayashi, SEPAC data base product tape, ISAS Research Note 283, Tokyo, Japan, March 1985.

# SEPAC

Space Experiment with Particle Accelerators

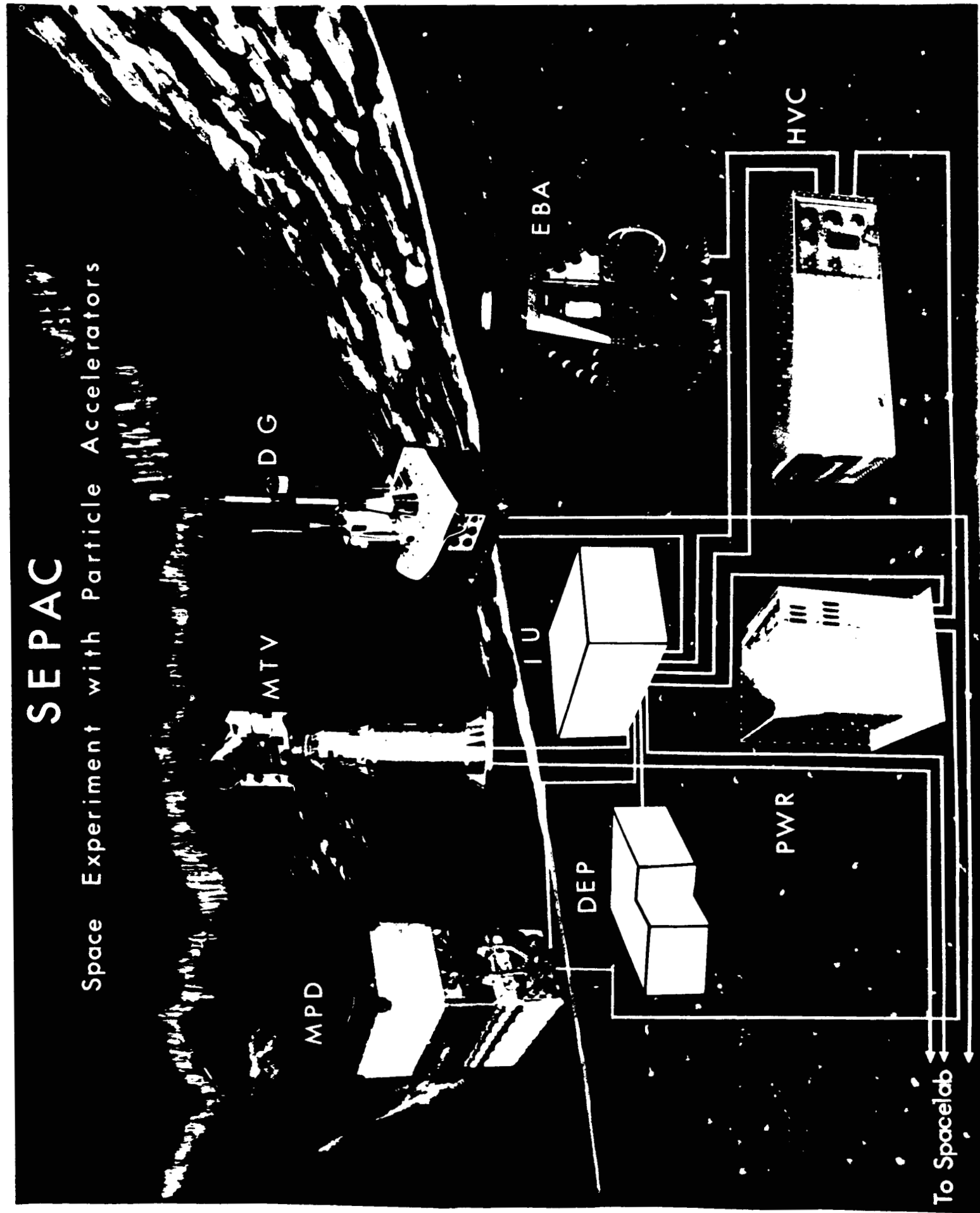
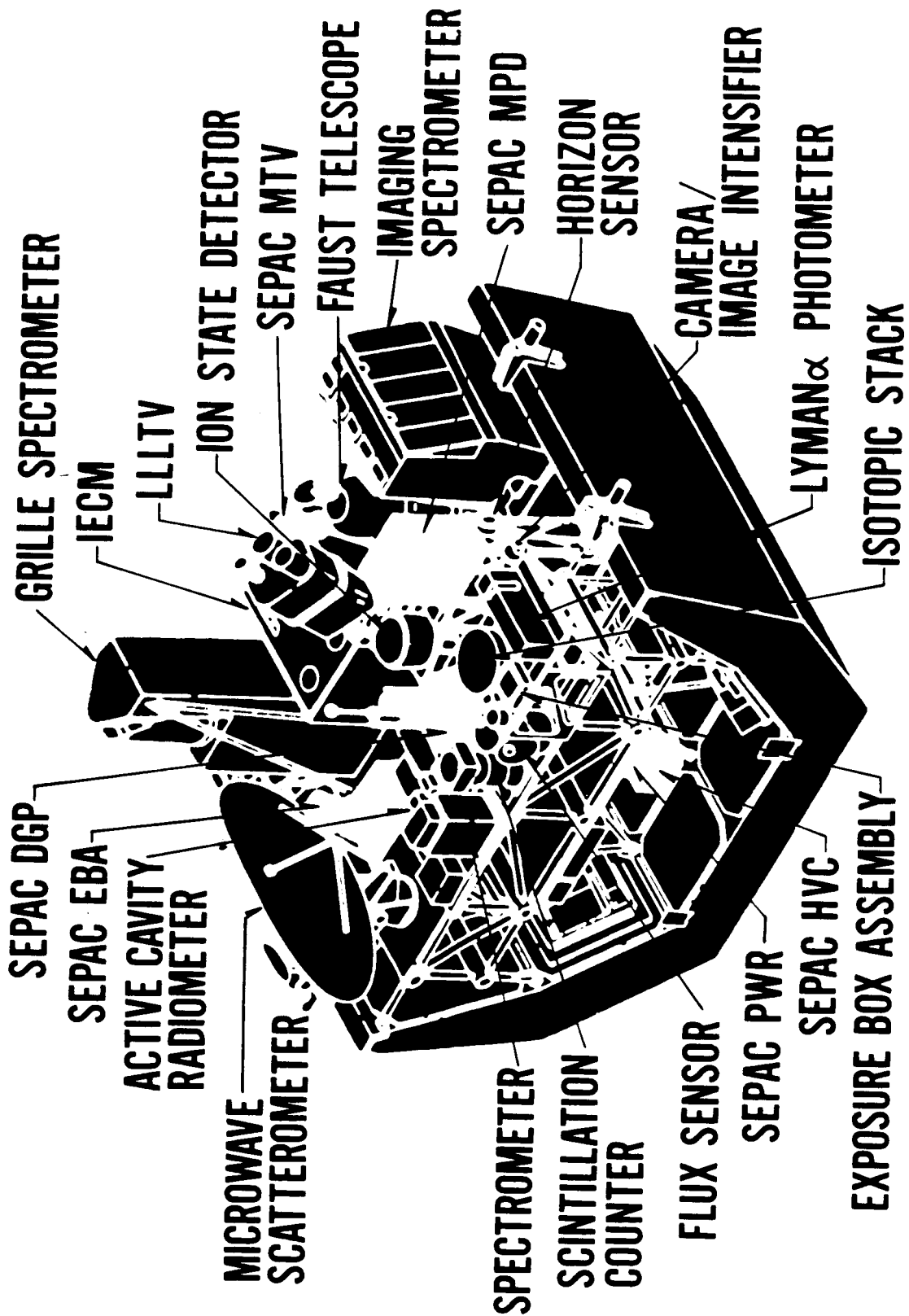


FIG 1



ORIGINAL PAGE IS  
OF POOR QUALITY

FIG 2

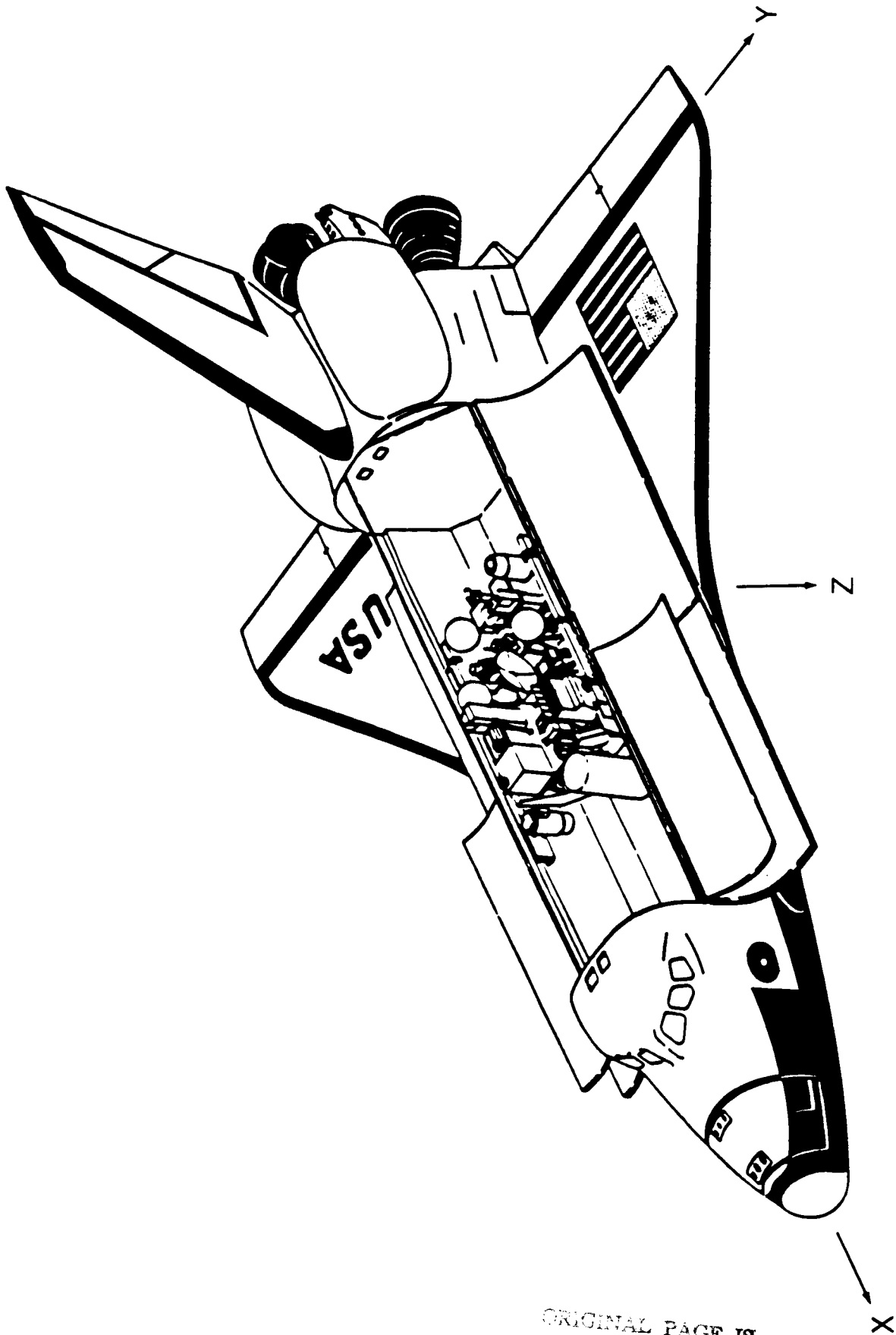


FIG 3

ORIGINAL PAGE IS  
OF POOR QUALITY

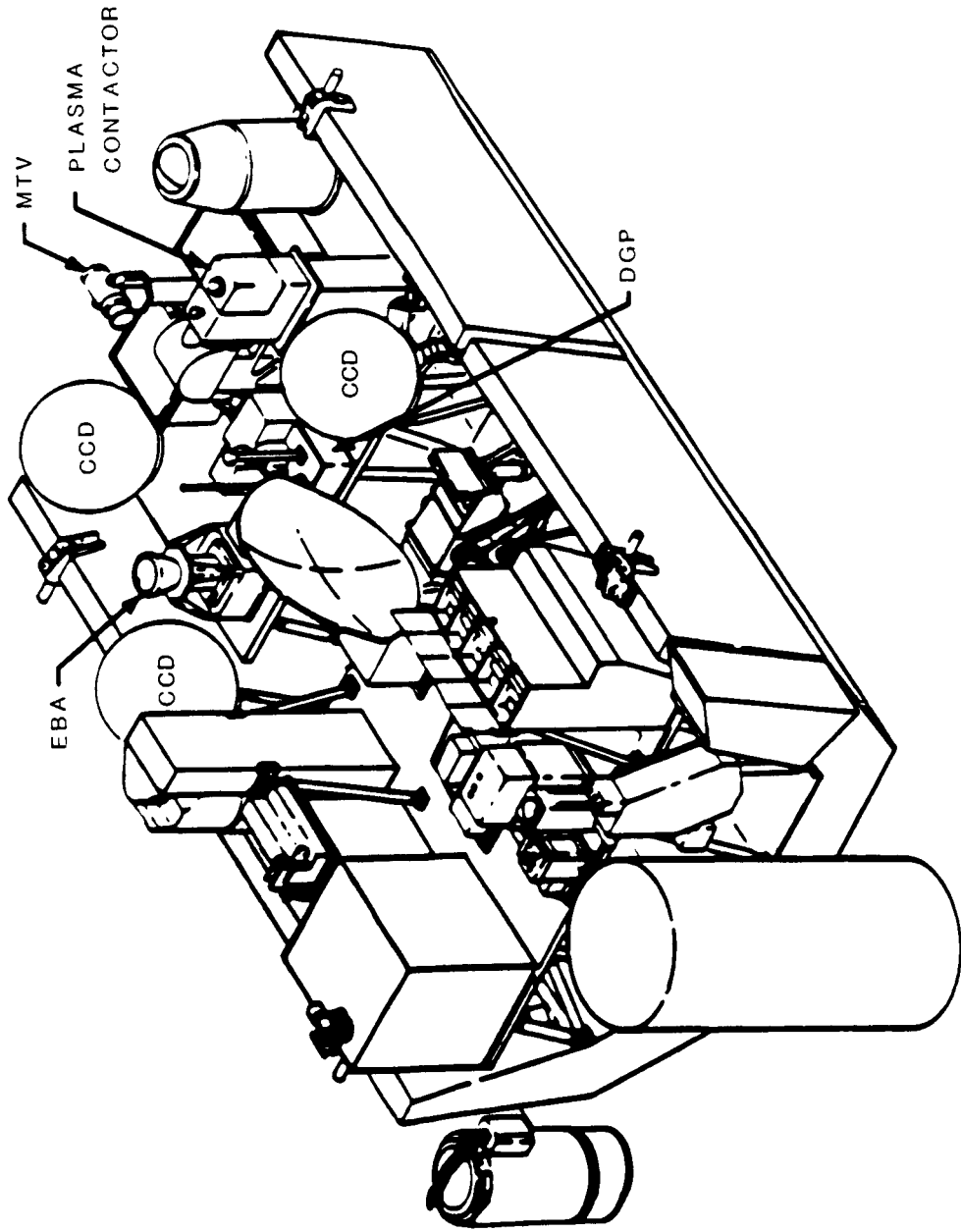


FIG 4

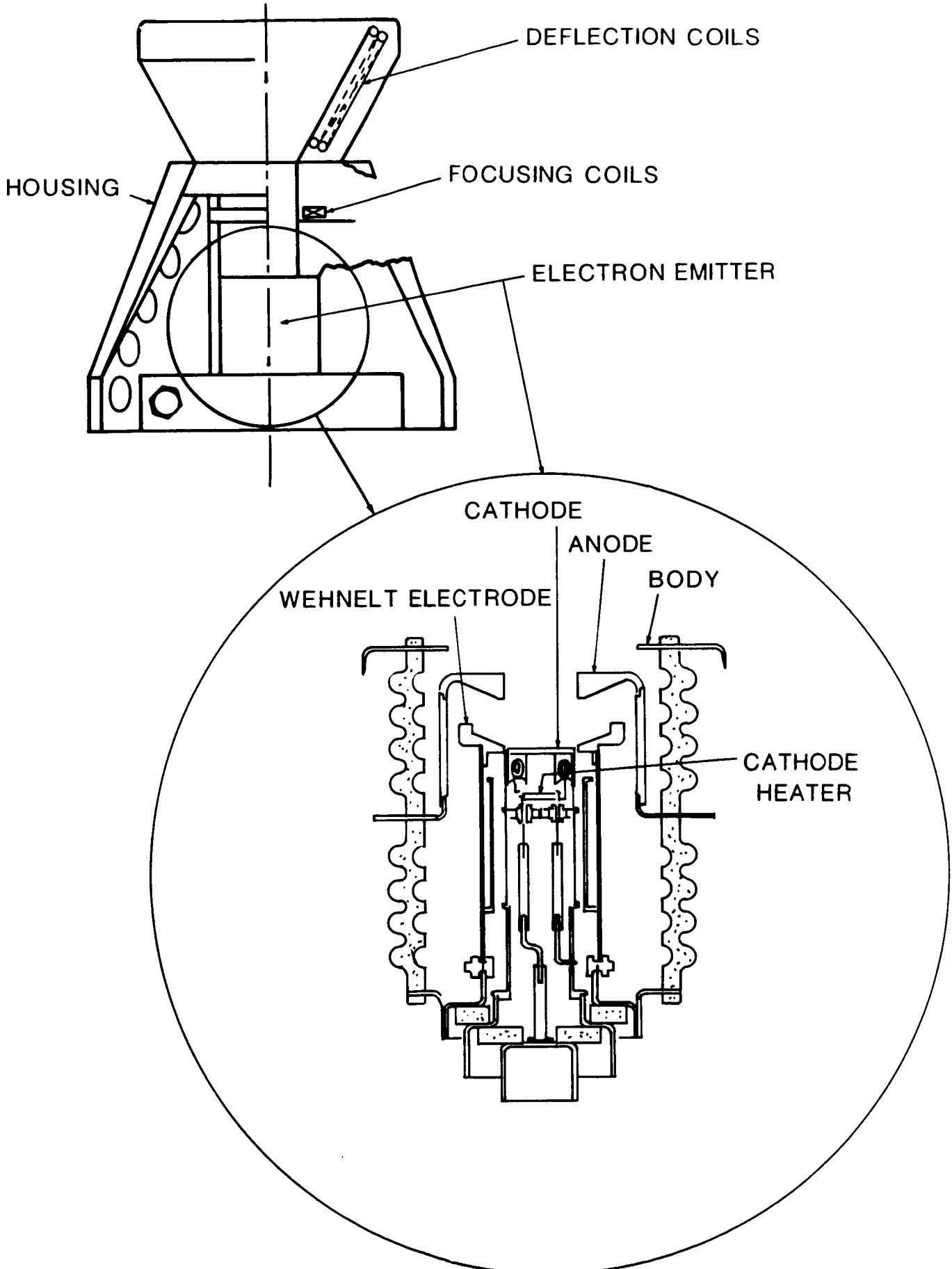
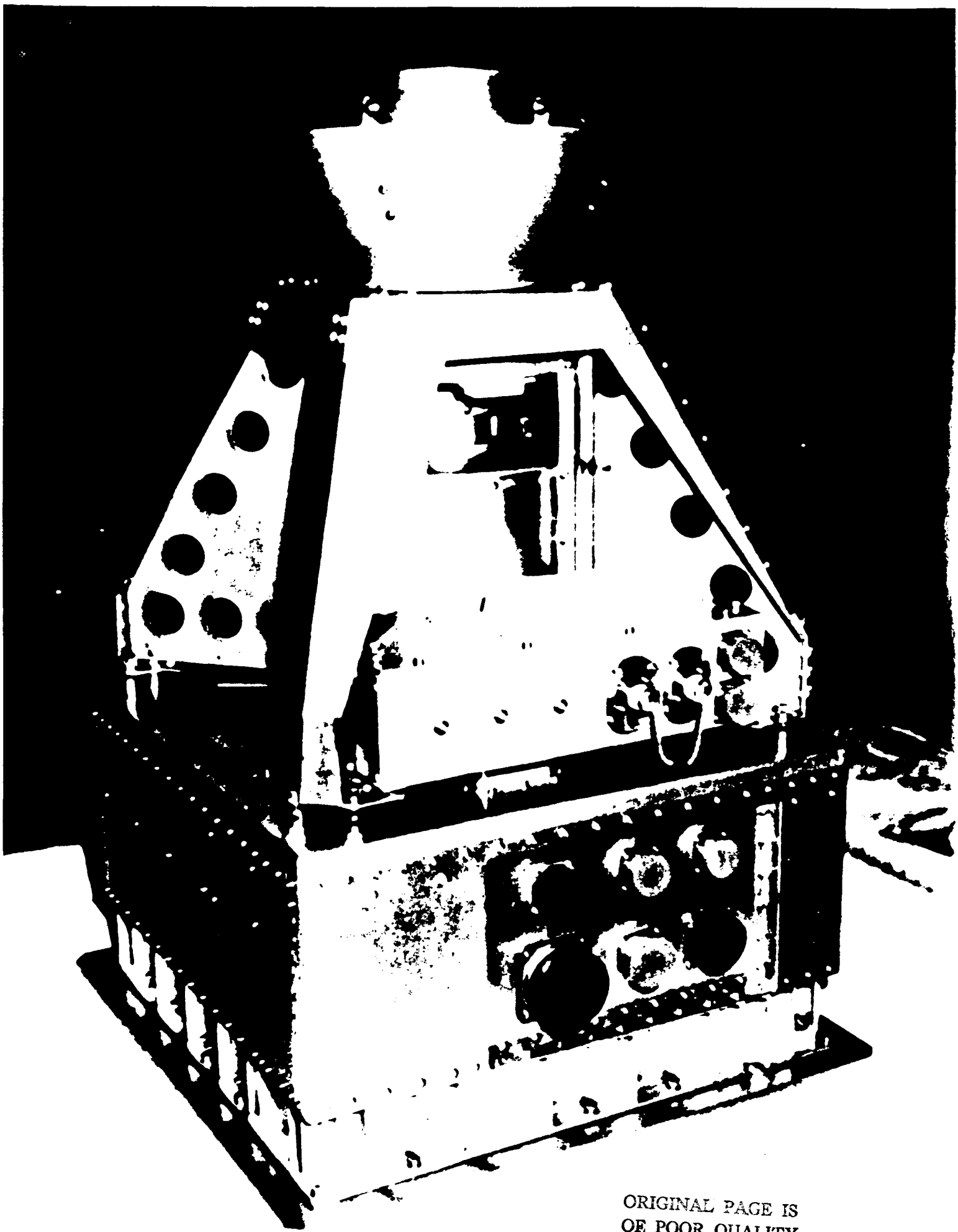


FIG 5



ORIGINAL PAGE IS  
OF POOR QUALITY.

FIG 6

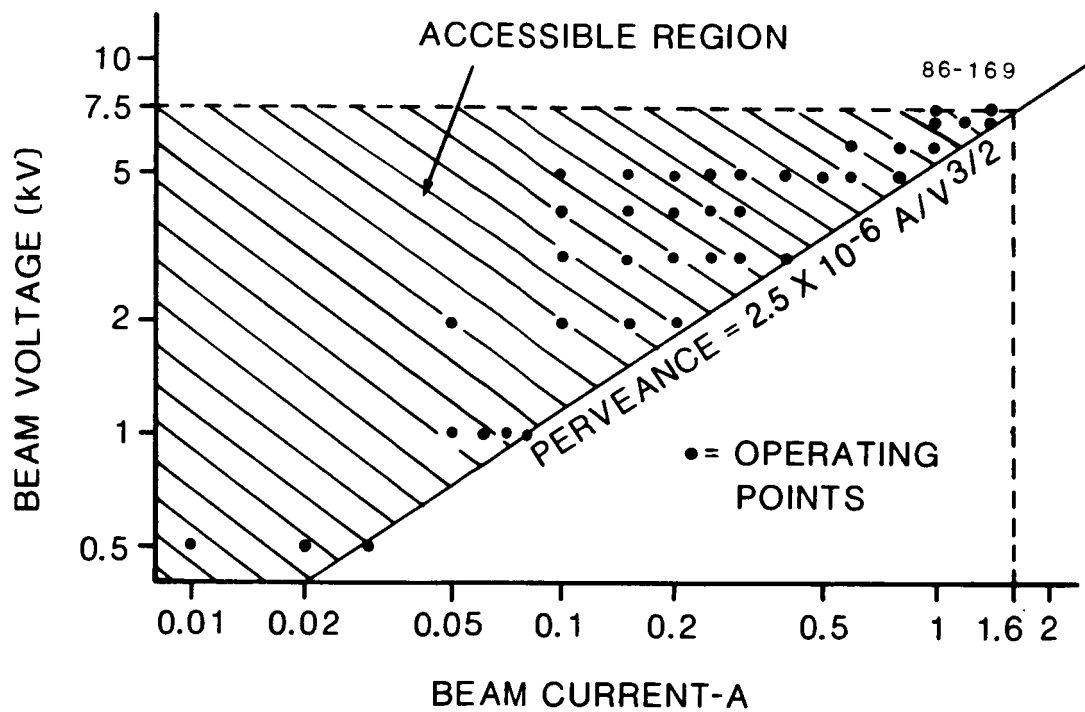


FIG 7

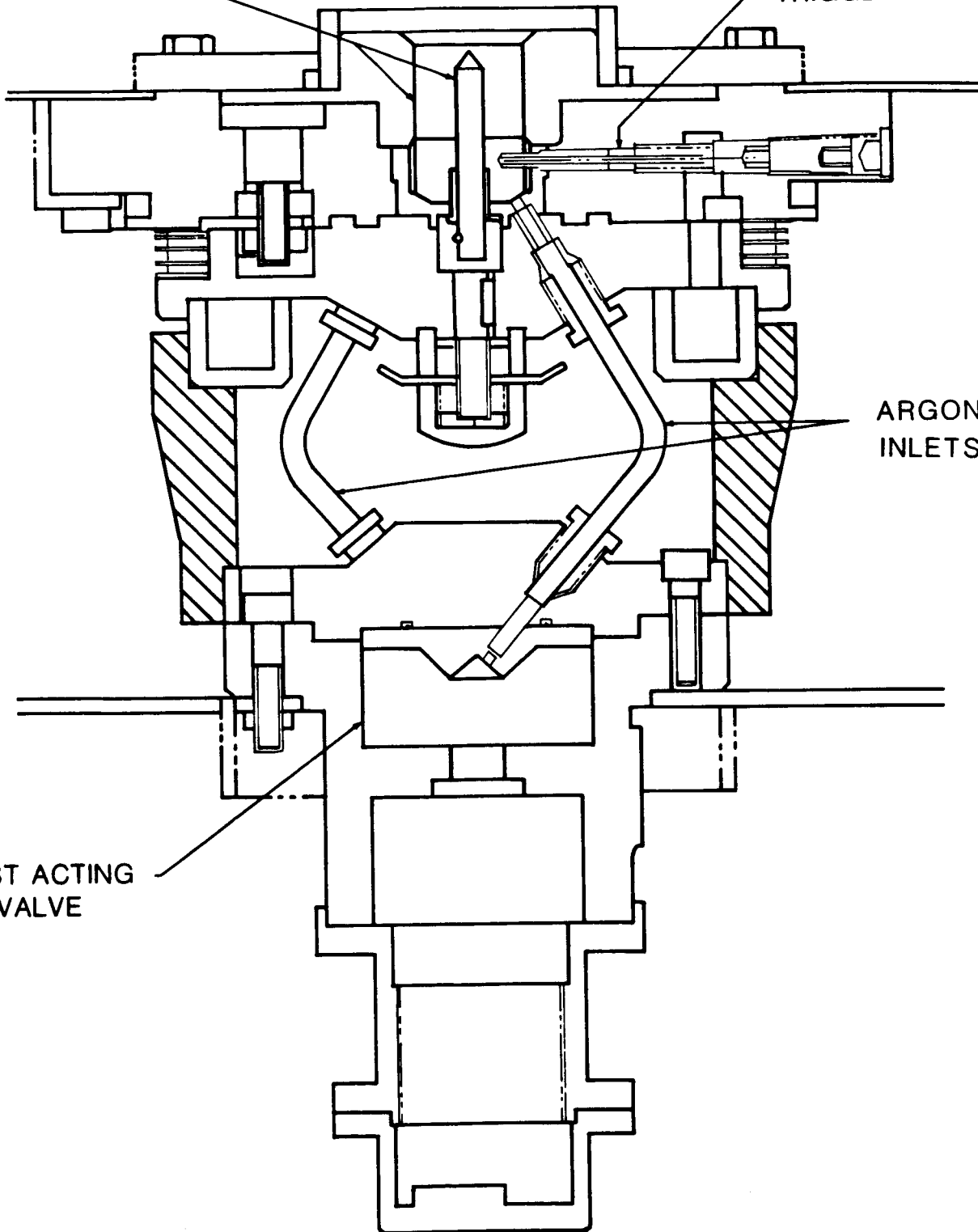
100 mm

SCALE:

86-166

MAIN ELECTRODES

TRIGGER ELECTRODE



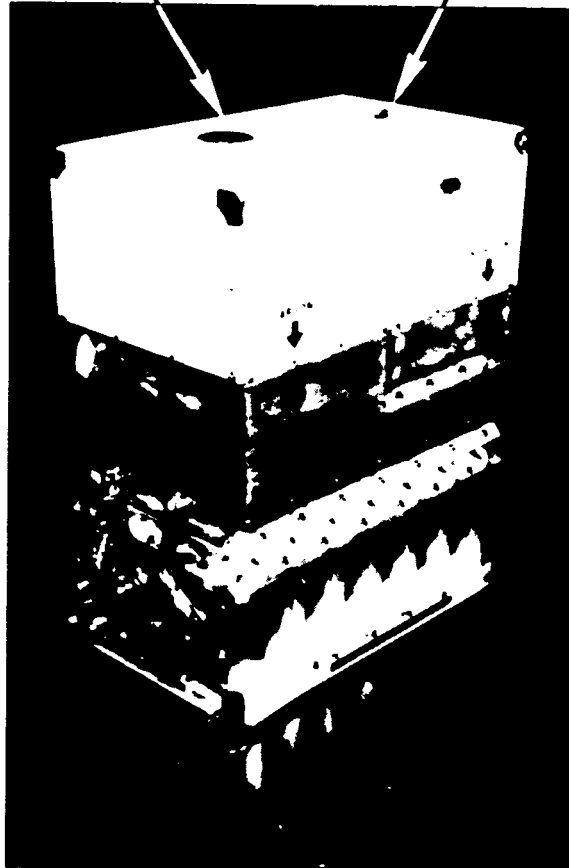
ARGON  
INLETS

FAST ACTING  
VALVE

FIG 8

MPD-AJ ELECTRODES

NGP NOZZLE



ORIGINAL PAGE IS  
OF POOR QUALITY

FIG 9

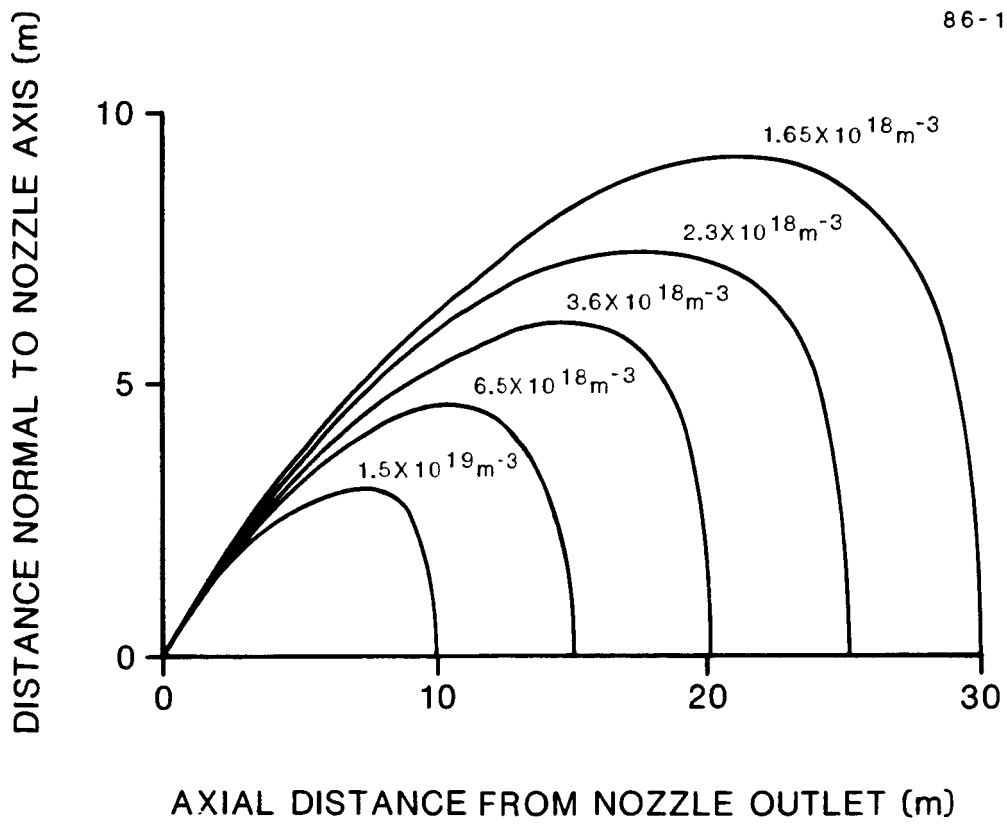


FIG 10

ORIGINAL PAGE IS  
OF POOR QUALITY

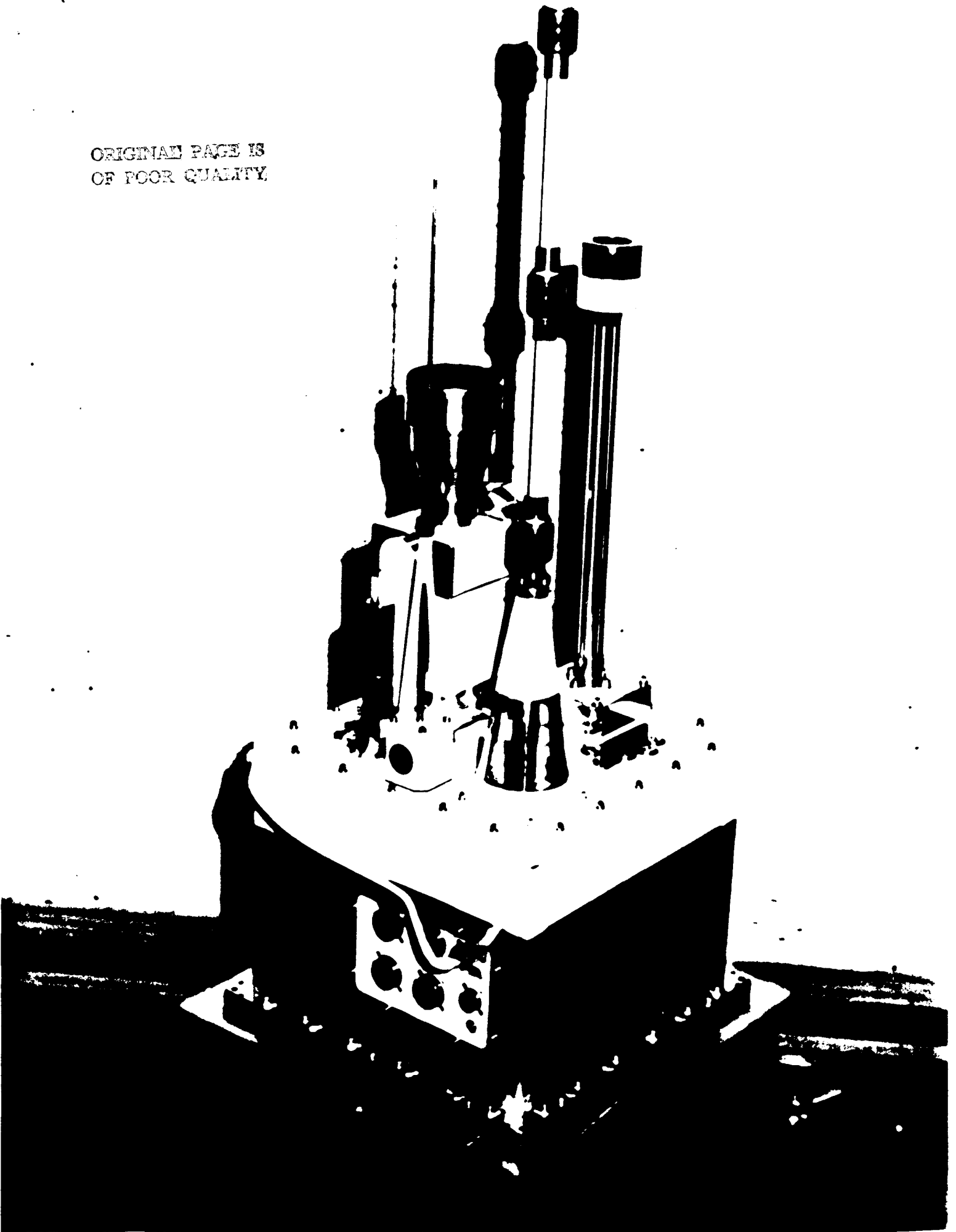


FIG 11

86-168

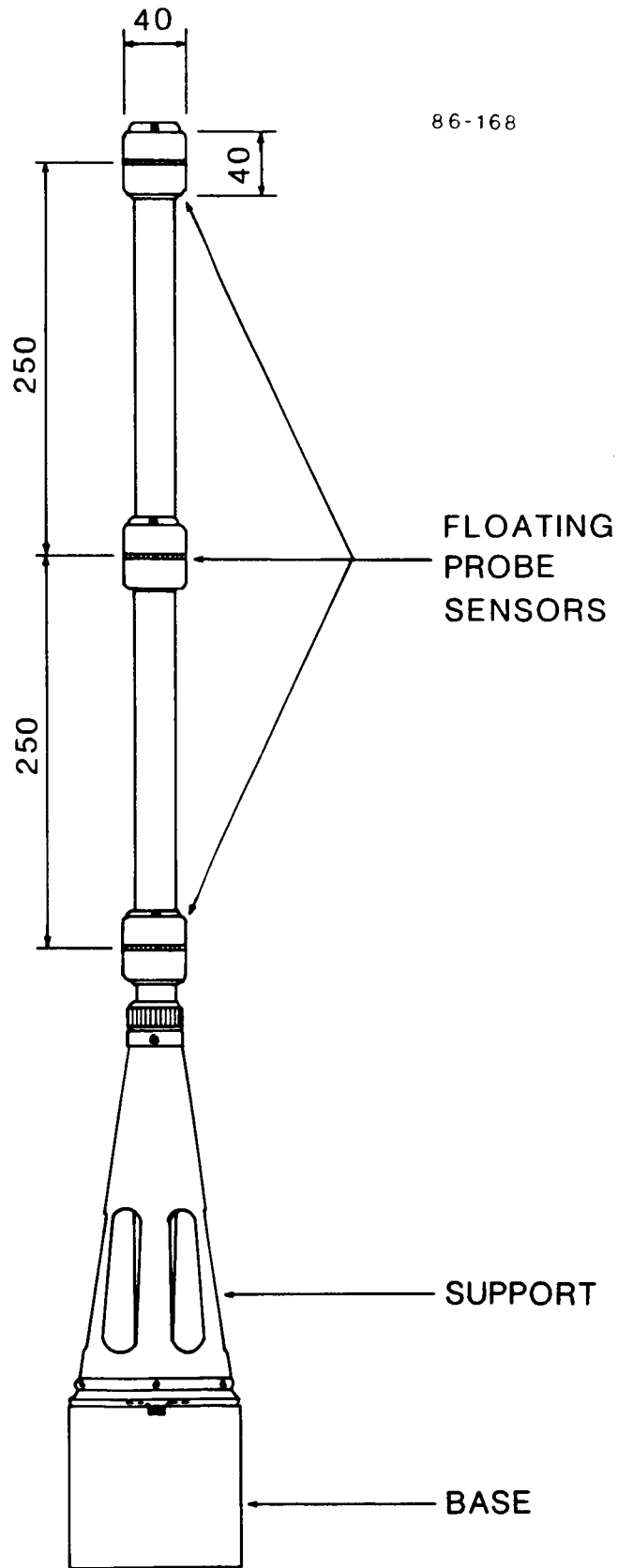


FIG 12

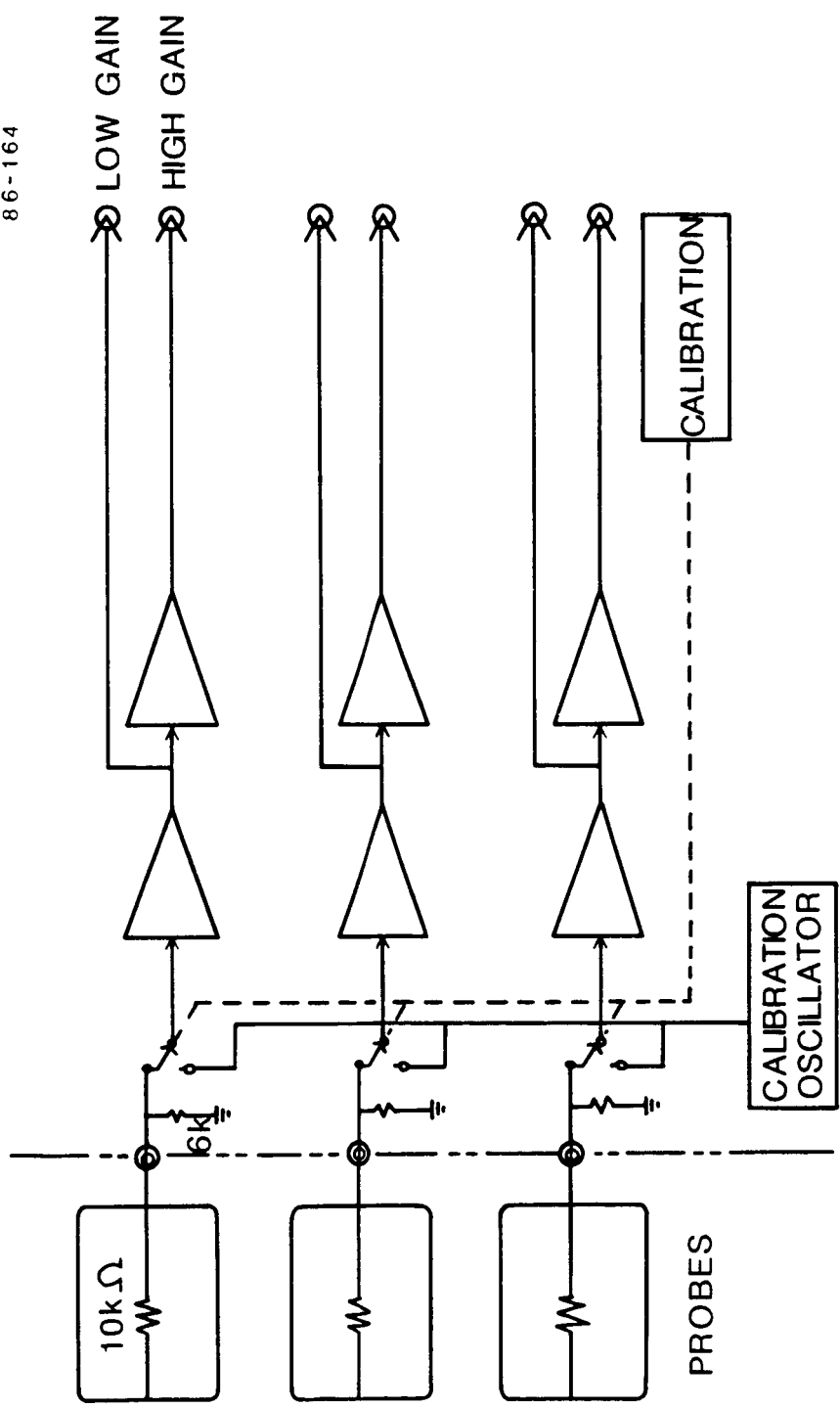


FIG 13

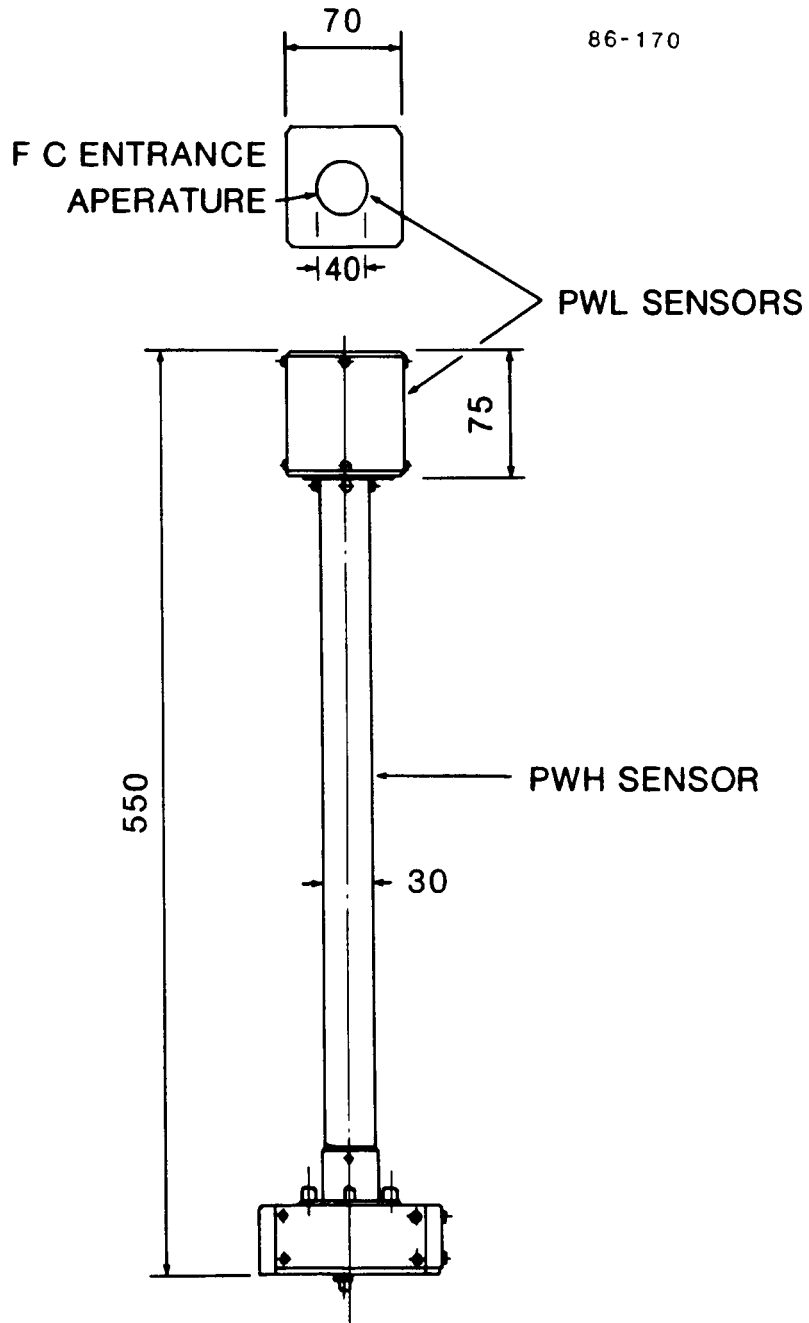


FIG 14

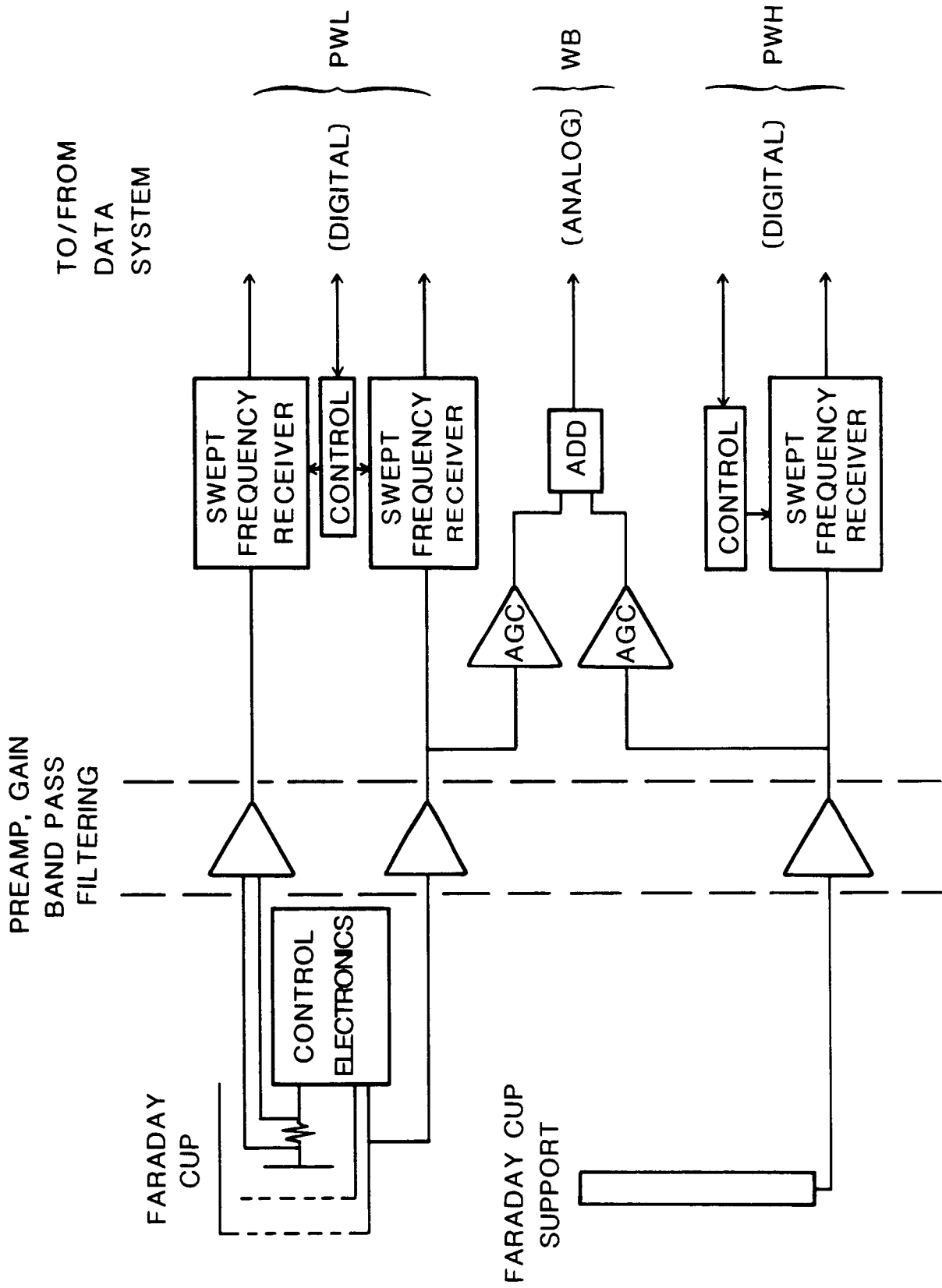


FIG 15

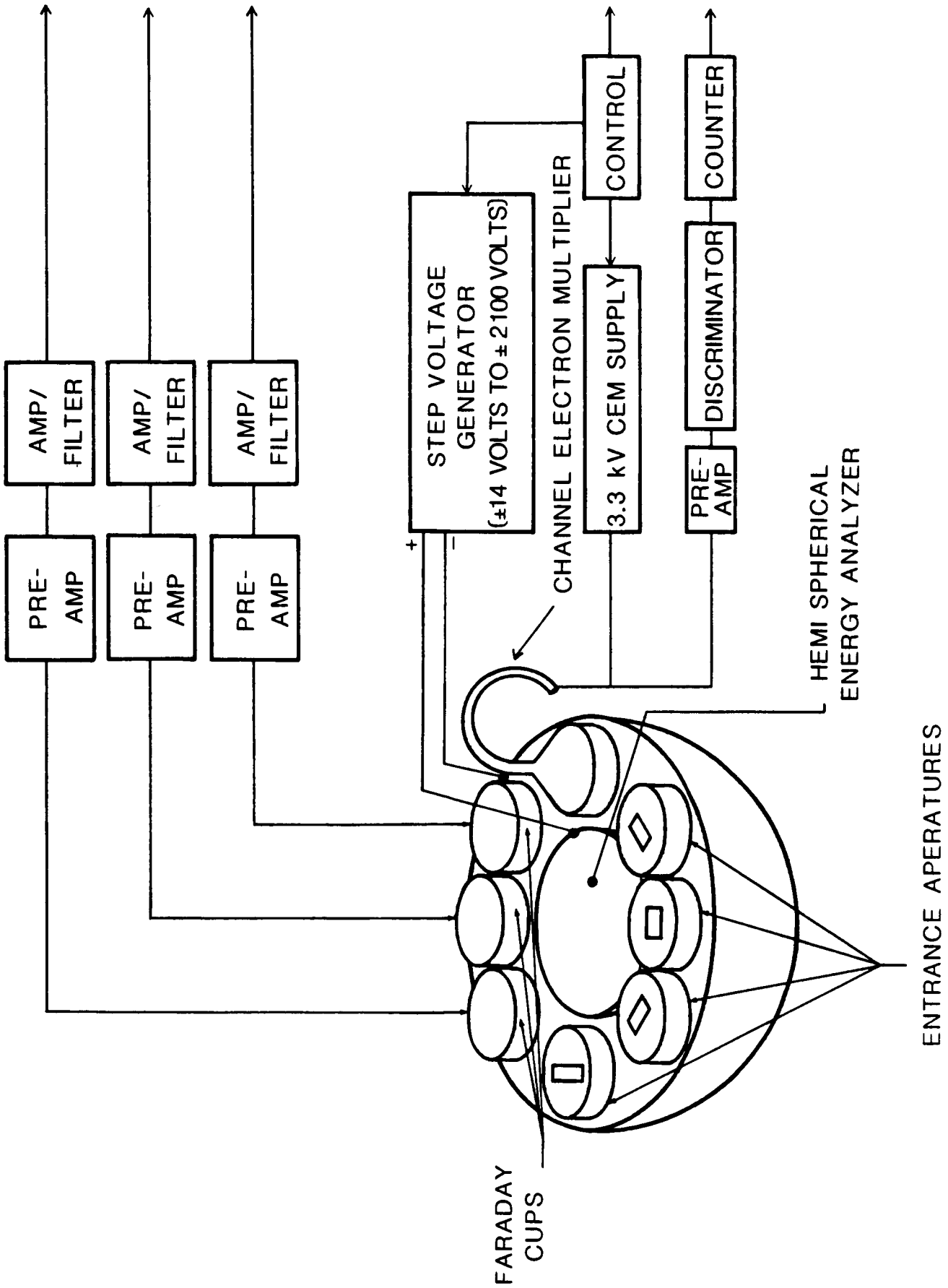


FIG 16

86-173

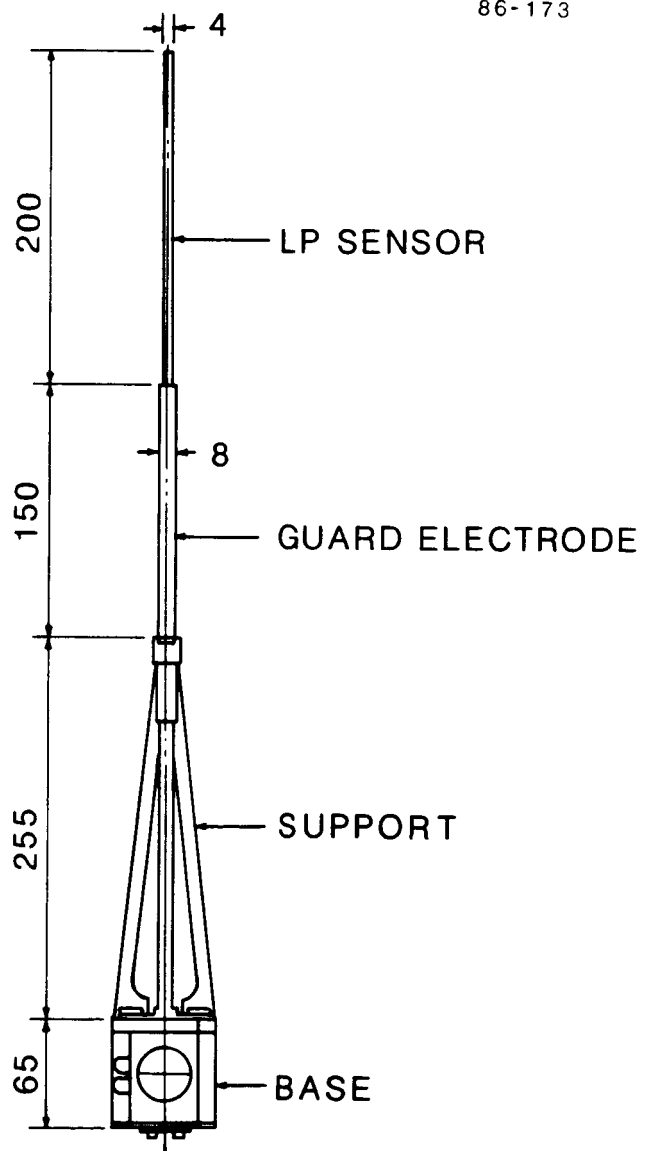


FIG 17

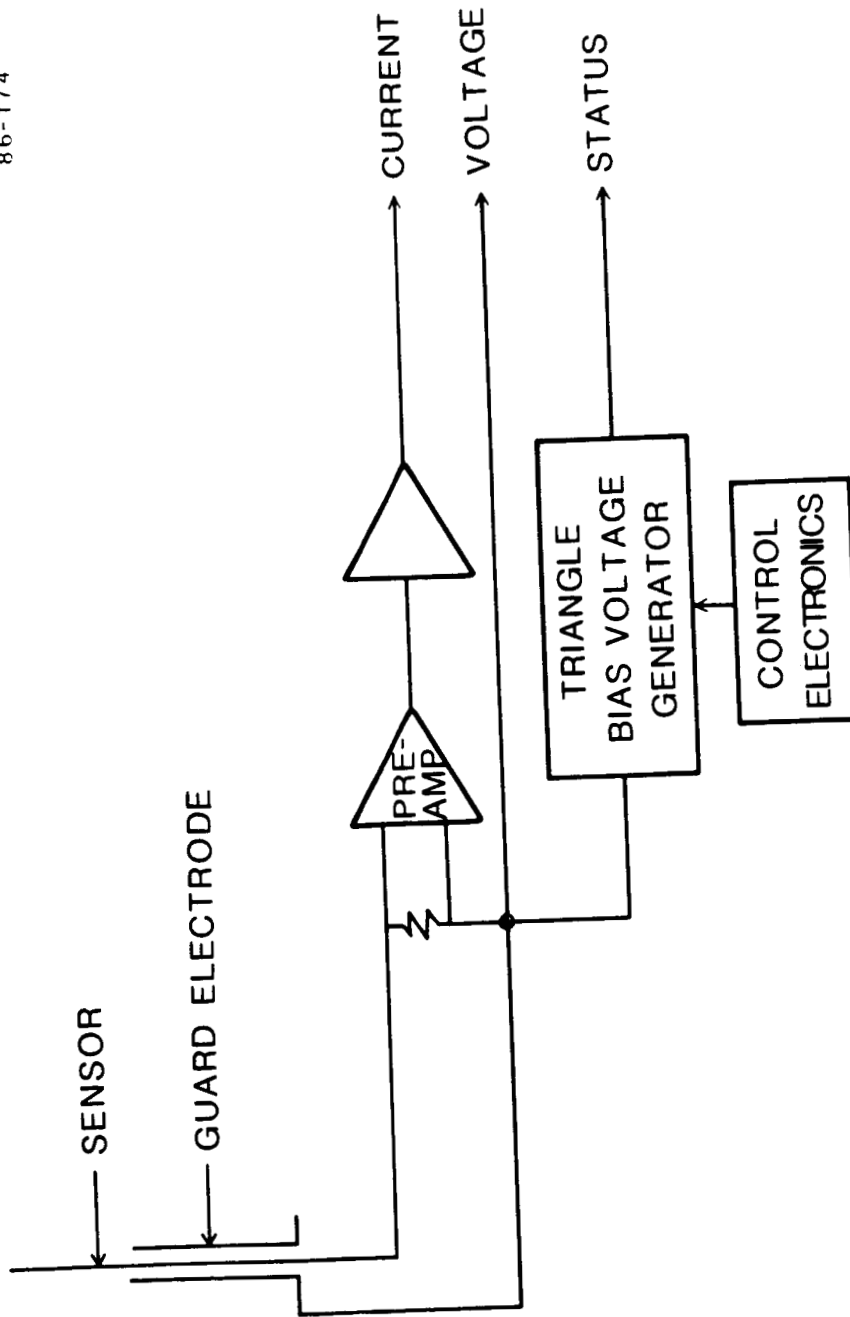


FIG 18

ORIGINAL PAGE IS  
OF POOR QUALITY

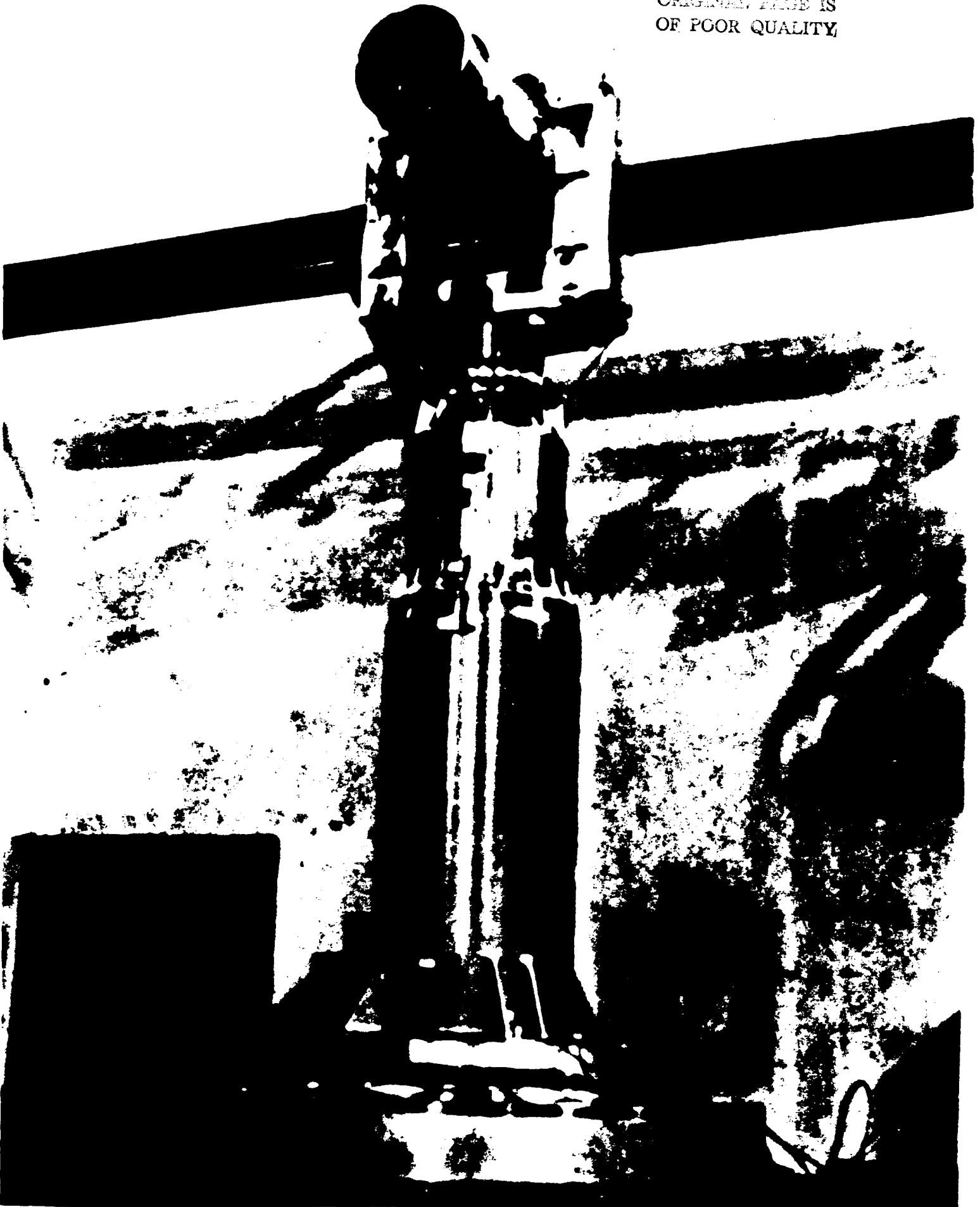


FIG 19

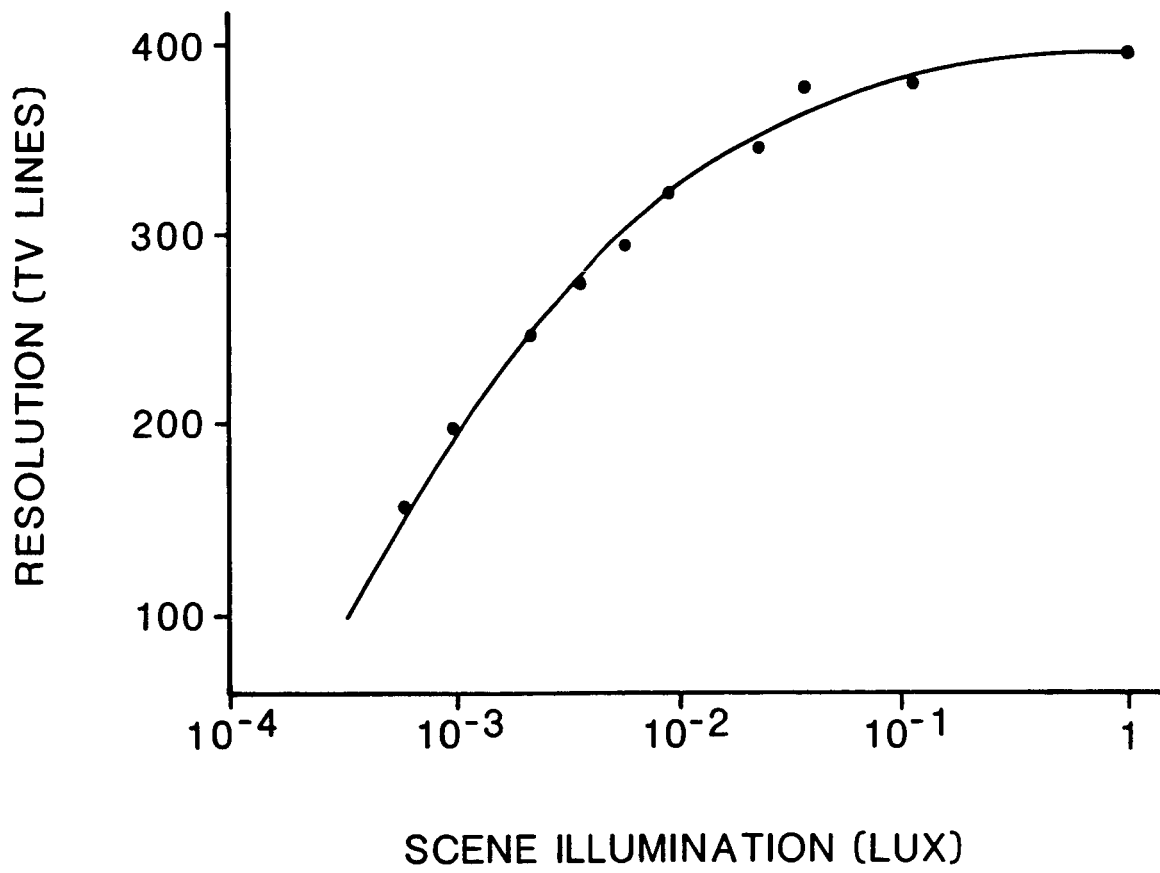


FIG 20

SPACELAB PALLET

SPACELAB MODULE

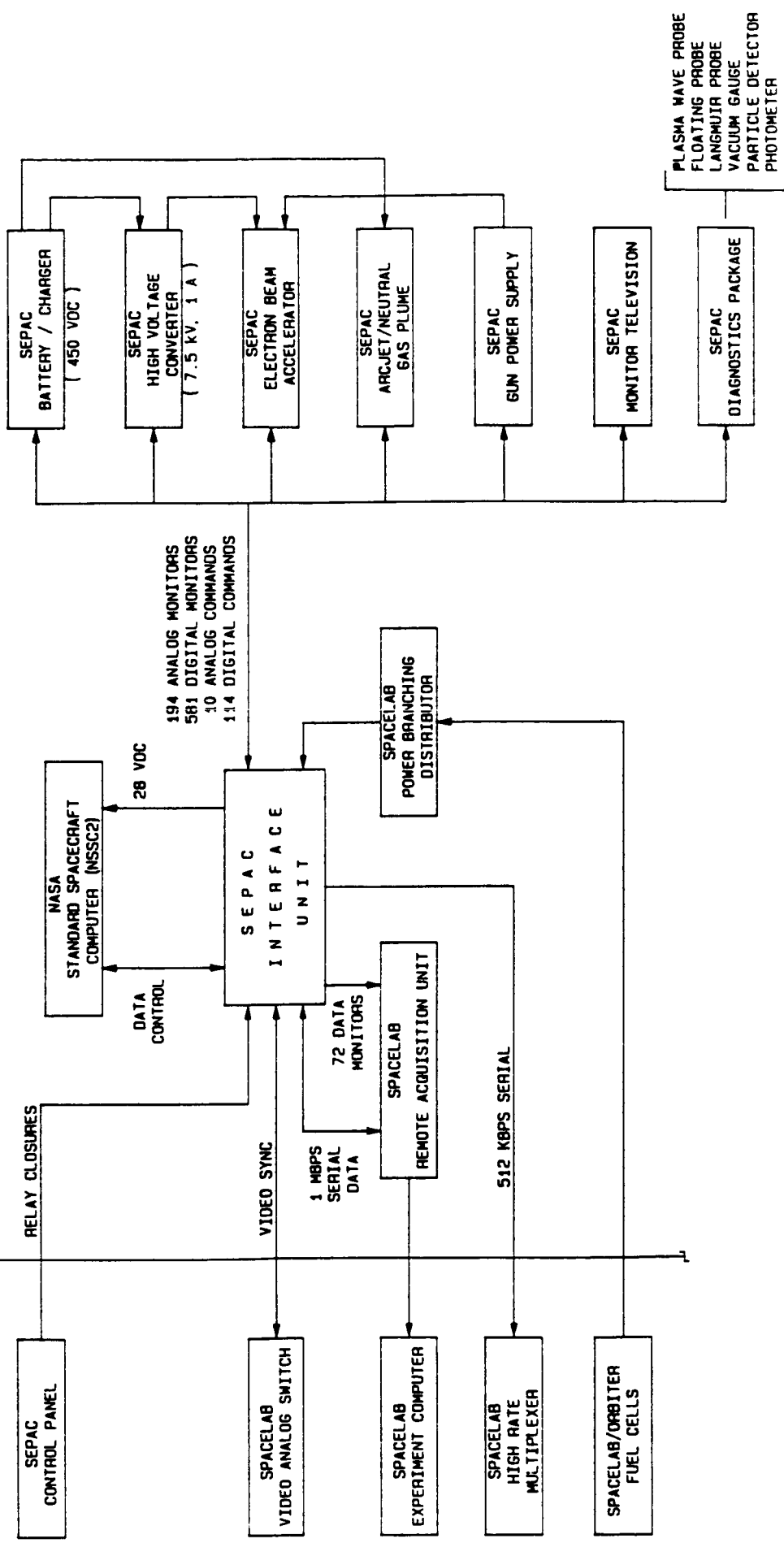
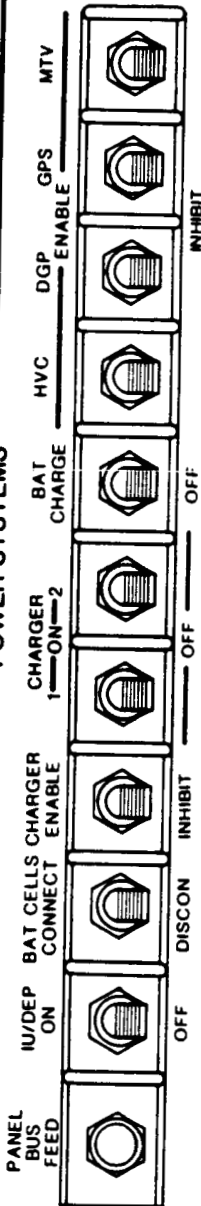


FIG 21

SEPAC

POWER SYSTEMS



MONITOR TV SYSTEMS

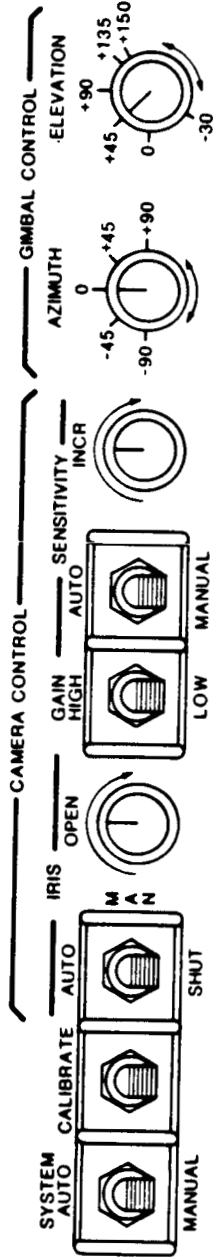


FIG 22

ORIGINAL PAGE IS OF POOR QUALITY